Pathogenic, but not non-pathogenic, *Rickettsia* evade inflammasome-dependent IL-1 responses to establish an intracytosolic replication niche.

Oliver H. Voss[1,*], Jennifer Cobb[1], Hodalis Gaytan, Natalia Rivera Díaz[2], Rigoberto Sanchez[2], Louis DeTolla[2], M. Sayeedur Rahman[1], Abdu F. Azad[1,*]

[1]Department of Microbiology and Immunology, University of Maryland School of Medicine, Baltimore, MD 21201, USA

[2]Department of Pathology, Comparative Medicine (Infectious Diseases), and Epidemiology and Public Health, University of Maryland School of Medicine, Baltimore, MD 21201, USA

*Correspondence: ovoss@som.umaryland.edu (O.H.V.), aazad@som.umaryland.edu (A.F.A.)

Keywords: *R. typhi*, *R. rickettsii* (*Sheila Smith*), *R. montanensis*, IL-1α, IL-1β, Caspase-1, Caspase-11, macrophages, inflammasomes.

Author Contributions

O.H.V., M.S.R., and A.F.A. planned the research, analyzed, and interpreted the data; O.H.V., J.C., H.G., N.R.D., and M.S.R. performed the experiments; A.F.A., O.H.V., L.D., and R.S. contributed to the overall project administration and supervision; O.H.V., M.S.R., and A.F.A. wrote the manuscript; and all authors participated in editing the manuscript.

ABSTRACT

Rickettsia species (spp.) are strict obligate intracellular bacteria, with some being pathogenic in their mammalian host, including humans. One critical feature of these stealthy group of pathogens is their ability to manipulate hostile cytosolic environments to their benefits. Although our understanding of *Rickettsia* cell biology and pathogenesis are evolving, the mechanisms by which pathogenic *Rickettsia* spp. evade host innate immune detection remains elusive. Here, we showed that disease severity in wild-type (*WT*) C57BL/6J mice infected with *R. typhi* (etiologic agent of murine *typhus*) and *R. rickettsii* (etiologic agent of Rocky Mountain Spotted Fever), but not with non-pathogenic *R. montanensis*, correlated with levels of bacterial burden as detected in the spleens, as well as the serum concentrations of pro-inflammatory cytokine IL-1α and to a lesser extent IL-1β. Antibody-mediated neutralization of IL-1α confirmed a key role in controlling mortality rates and bacterial burdens of rickettsiae-infected *WT* mice. As macrophages are a primary source of both IL-1α and IL-1β cytokines, we determined the mechanism of the anti-rickettsial activities using bone-marrow-derived macrophages. We found that pathogenic *R. typhi* and *R. rickettsii*, but not non-pathogenic *R. montanensis*, eluded pro-IL-1α induction and benefited pre-dominantly from the reduced IL-1α secretion, via a Caspase-11-Gsdmd-dependent pathway, to facilitate intracytosolic replication. Adoptative transfer experiments identified that IL-1α secretion by macrophages was critical for controlling rickettsiosis in *WT* mice. In sum, we identified a previously unappreciated pathway by which pathogenic, unlike non-pathogenic, rickettsiae

46 preferentially target the Caspase-11-Gsdmd-IL-1α signaling axis in macrophages thus
47 supporting their replication within the host.
48
49 **IMPORTANCE**
50 Currently, no vaccines are available to prevent rickettsioses, while vector-borne
51 rickettsial infections in humans are on the rise globally. In fact, the insufficient
52 understanding of how pathogenic *Rickettsia* species circumvent host immune defense
53 mechanisms has significantly hindered the development of more effective therapeutics.
54 Here, we identified a previously unappreciated role for the Caspase-11-Gsdmd-IL-1α
55 signaling axis, to limiting the replication of pathogenic *R. rickettsia* and *R. typhi* species
56 in murine macrophages and wild-type (*WT*) C57BL/6J mice. Adoptative transfer studies
57 further identified IL-1α-secreting macrophages as critical mediators in controlling
58 rickettsial infection in *WT* mice. Collectively, these findings provide insight into the
59 potential mechanism of how pathogenic, but not non-pathogenic *Rickettsia* spp., benefit
60 from a reduction in the Caspase-11-Gsdmd-mediated release of IL-1α to support host
61 colonization.
62
63 **INTRODUCTION**
64 Invasive cytosolic bacteria, including *Listeria*, *Shigella*, *Burkholderia*, *Francisella*,
65 *Orientia*, and *Rickettsia* species (spp.) have developed strategies to induce their own
66 uptake by phagocytosis and to circumvent host innate immune defenses for their
67 intracellular survival (1, 2). Human infection with *Rickettsia* spp. occurs via infected
68 hematophagous arthropods such as fleas, ticks, and human body lice (3), either through
69 the bite or deposited infected feces into skin and mucosal surfaces. Upon entry, *Rickettsia*

70 spp. encounter tissue-resident immune cells, like macrophages (MΦ). Activated MΦ play
71 a crucial role in either terminating an infection at an early stage, which commonly is the
72 fate of non-pathogenic *Rickettsia* spp., or succumbing to bacterial replication and
73 pathogen colonization as well as host dissemination to distant organs (3). After
74 internalization into host cells, *Rickettsia* spp. escape from phagosomes and subvert host
75 cytosolic defense mechanisms (*i.e.*, autophagy and inflammasomes) to establish an
76 intracytosolic replication niche. Recently, we reported that pathogenic *Rickettsia* spp.
77 secret effectors to promote host colonization by modulating endoplasmic reticulum
78 structures or by hijacking the autophagic defense pathway (4–9). Subversion of
79 autolysosomal destruction to colonize the host cytosol exposes *Rickettsia* spp. to another
80 cytosolic host sensor-regulated defense mechanism, the inflammasomes (1, 10).
81 Inflammasomes are immune signaling complexes categorized into canonical [Caspase
82 (Casp)-1] and non-canonical [murine Casp-11 or human Casp-4/5] inflammasomes. The
83 inflammasome complex assembly involves the adaptor protein ASC and upstream
84 sensors including NLRP1, NLRP3, NLRC4, AIM2, and pyrin, which are primed by
85 exogenous pathogen-associated molecular pattern molecules (PAMPs) and activated
86 through endogenous damage-associated molecular pattern molecules (DAMPs).
87 Initiation of the canonical inflammasome results in the activation of Casp-1. Active Casp-
88 1 leads to the maturation of proinflammatory cytokines IL-1β and IL-18 and the activation
89 of gasdermin D (Gsdmd), the executor of pyroptosis (11, 12). Of note, recent findings
90 have also suggested that active Casp-11 is capable of activating Gsdmd (11, 12).
91 Although IL-1β is released by both canonical and non-canonical inflammasome
92 pathways, IL-1α is preferentially released by the non-canonical inflammasome pathway

93 (13–15). IL-1α is expressed by a wide range of hematopoietic and non-hematopoietic cell
94 types, whereas IL-1β is primarily produced by myeloid cells (15). Importantly, although
95 IL-1α and IL-1β signal through the same receptor, IL-1R, these two cytokines are not
96 completely functionally redundant (15). Given the importance for both canonical and non-
97 canonical inflammasome-mediated IL-1 signaling in limiting pathogen colonization, many
98 bacteria have evolved strategies to block their activation (16–21). In fact, various
99 pathogenic intracellular bacteria utilize their own effector repertoire to evade these
100 pathways to successfully colonize and disseminate in their host cells (10, 22).

101 In the case of *Rickettsia*, our understanding of the role of inflammasomes in controlling
102 host colonization is only now emerging (23–25). Specifically, how pathogenic *Rickettsia*
103 spp. manipulate immune defenses to replicate within the host cytosol not only relies
104 almost exclusively on data from tick-transmitted rickettsiae [*e.g.*, members of spotted
105 fever group (SFG) or transition group (TRG)], but also shows that these pathogens likely
106 employ species-specific strategies to evade host cytosolic defense mechanisms. For
107 instance, *R. australis*, a pathogenic TRG member, benefited from ATG5-mediated
108 autophagy induction and suppression of inflammasome-dependent IL-1β production to
109 colonize both BMDMΦ (23) and mice (26). In contrast, *R. parkeri*, a mildly pathogenic
110 member of SFG (see Fig. 1A), utilizes its surface cell antigen Sca5 (OmpB) for protection
111 against autophagic recognition, and consequently benefits from inflammasome-mediated
112 host cell death that antagonizes the action of Type I IFN in BMDMΦ and mice (24, 27). In
113 contrast, our recent report on the flea-transmitted *R. typhi* [pathogenic member of typhus
114 group (TG)], showed that *R. typhi* is ubiquitinated upon host entry and escapes
115 autolysosomal fusion to establish an intracytosolic niche in non-phagocytic cells (9).

116 These unexpected findings on how members of SFG, TRG, and TG *Rickettsia*
117 differentially promote intracytosolic host survival prompted us to explore the underlying
118 mechanism(s) by which pathogenic, but not non-pathogenic *Rickettsia* spp., block
119 immune defense responses to establish a replication niche in phagocytic cells, like MΦ.
120 Specifically, we sought to test the hypothesis that pathogenic, but not non-pathogenic,
121 *Rickettsia* spp. reduce inflammasome-mediated IL-1 responses thereby promoting their
122 intracytosolic replication within host cells.
123

124 **RESULTS**

125 ***In vivo* models of rickettsiosis**.

126 At present, more than 30 *Rickettsia* spp. have been described globally, but less than
127 a dozen is known to cause disease in humans, with some being notoriously pathogenic
128 and associated with high morbidity and mortality, while others exert limited or no
129 pathogenicity (Fig. 1A). We sought to test our hypothesis that pathogenic, but not non-
130 pathogenic, *Rickettsia* spp. evade immune responses in host defense cells, like MΦ, to
131 replicate and disseminate. We simultaneously evaluated the cytosolic host defense
132 responses between pathogenic [*R. rickettsii* (*Sheila Smith, SS*) and *R. typhi* (Wilmington)
133 and non-pathogenic (*R. montanensis*) strains *in vivo*. We first established a mouse model
134 of mild (~LD_{25}) or more severe (~LD_{50}) rickettsiosis in C57BL/6J *WT* mice. For both *R.*
135 *rickettsii* and *R. typhi* LD_{25} or LD_{50} were achieved with doses of 10^5 or 10^6 PFU,
136 respectively (Figs. 1B-C), however, *R. montanensis*-infected mice showed no signs of
137 lethality at either 10^5 or 10^6 PFU (Fig. 1D). Bacterial burden in spleens from infected
138 C57BL/6J *WT* mice (only dose of 10^6 PFU is shown) confirmed successful infection with

139 all three *Rickettsia* spp. at day 3 post-infection, while *R. typhi*- and *R. rickettsii*-infected
140 *WT* mice displayed significantly higher bacterial burden in the spleens as compared to
141 splenic tissues from *R. montanensis*-infected mice at day 7 (Fig. 1E). This correlated with
142 the observed differences in the spleen sizes and weights of the infected animals (Fig.
143 S1). Given the earlier findings from other laboratories and ours (9, 23–28), we
144 hypothesized that the observed dissimilarities in pathogenicity among *Rickettsia* spp. is
145 likely linked to differences in host defense responses. Recent findings further suggest
146 that the intracytosolic survival of different *Rickettsia* spp. is either supported or
147 suppressed by immune defense responses (*e.g.*, IFN-I, TNF-α, or IL-1β) (23–28), and
148 thus leaving the precise mechanism to be determined. Therefore, we first sought to
149 evaluate immune defense responses at the level of IL-1β and IL-1α cytokine secretion in
150 the sera of *R. typhi*-, *R. rickettsii*-, and *R. montanensis*-infected animals. The increase in
151 mortality and elevated bacterial burden correlated with reduced serum levels of both IL-
152 1β and IL-1α cytokines (Figs. 1F-G), suggesting that reduced activation of both IL-1
153 signaling responses is a potential mechanism for lethality and survival of pathogenic
154 *Rickettsia* spp.
155
156 **Anti-rickettsial activity of IL-1α is involved in restricting *Rickettsia* infection.**
157 To characterize further the role of IL-1α and IL-1β cytokines in restricting non-
158 pathogenic and pathogenic *Rickettsia* spp. *in vivo*, IL-1α or IL-1β function was neutralized
159 via tail vein (*i.v.*) injection, with anti(α)-IL-1α, αIL-1β, or αIgG-isotype control antibodies
160 (Abs) into C57BL/6J *WT* mice in our established model of mild rickettsiosis (LD_{25}; ~10^5
161 PFU, Figs. 1B-D). Neutralization of IL-1α, and to a much lesser extent IL-1β, was

162 associated with a significant increase in the mortality of *R. typhi*-, *R. rickettsii*-, and *R.*
163 *montanensis*-infected mice (Figs. 2A-C) and resulted in the development of splenomegaly
164 (Fig. S2), which correlated with an increase in bacterial loads in the spleen (Fig. 2D). The
165 efficiency of Ab-mediated blocking was confirmed by measuring the levels of IL-1β and
166 IL-1α cytokine in the sera of the rickettsiae-infected mice (Figs. 2E-F). Next, we sought to
167 determine the effect of administering recombinant (r)IL-1α or rIL-1β proteins on *Rickettsia*
168 colonization *in vivo*. Accordingly, we administered (*i.v.*) endotoxin-free rIL-1α and rIL-1β
169 proteins following infection with *R. typhi*, *R. rickettsii*, and *R. montanensis*. Pretreatment
170 of mice with rIL-1α, and to a lesser extent rIL-1β, protected C57BL/6J *WT* mice from
171 pathogenic *Rickettsia*-induced lethality (Figs. 3A-C), with both reduced splenomegaly
172 (Fig. S3), and decreased splenic bacterial burdens (Fig. 3D). Moreover, the observed
173 phenotypes correlated with the measured IL-1α and IL-1β serum concentrations (Figs.
174 3E-F). Collectively, these findings suggest that IL-1α, and to a lesser extent, IL-1β, are
175 involved in restricting the replication and colonization of non-pathogenic and pathogenic
176 *Rickettsia* spp. in C57BL/6J *WT* mice.
177

178 **Pathogenic, but not non-pathogenic, *Rickettsia* species block IL-1α secretion and**
179 **avoid pro-IL-1α induction to establish a replication niche in macrophages.**

180 As MΦ are one of the cell types first encountered during infection by *Rickettsia* spp.
181 and are considered to play a crucial role in either terminating the infection early at the
182 skin site or allow initial pathogen colonization and subsequent dissemination within the
183 infected host (3), we tested the hypothesis that pathogenic, but not non-pathogenic,
184 rickettsiae suppress MΦ immune responses. In this effort, we determine the importance

185 of IL-1α and IL-1β in restricting the replication of *Rickettsia* spp. by infecting BMDMΦ
186 derived from *WT*, *Il-1β*$^{-/-}$ or *Il-1α*$^{-/-}$ mice with pathogenic *R. typhi* and *R. rickettsii* or non-
187 pathogenic *R. montanensis* and assessed the cytokine levels of IL-1β and IL-1α in
188 cultured supernatants as well as bacterial burdens. Infection of *Il-1β*$^{-/-}$ or *Il-1α*$^{-/-}$ BMDMΦ
189 with *Rickettsia* spp. did not result in the secretion of either IL-1β or IL-1α, respectively,
190 when compared to infected *WT* BMDMΦ (Figs. 4A-F). Moreover, infections with *R.*
191 *montanensis* resulted in overall higher IL-1 responses and lower bacterial burden when
192 compared to infections performed with *R. typhi* or *R. rickettsii* in *WT*, *Il-1β*$^{-/-}$ or *Il-1α*$^{-/-}$
193 BMDMΦ (Figs. 4A-G). Of note, the bacterial burden of all three *Rickettsia* spp. in infected
194 *Il-1α*$^{-/-}$ BMDMΦ was higher than the levels detected in *Il-1β*$^{-/-}$ or *WT* BMDMΦ (Fig. 4G),
195 suggesting that IL-1α and to significantly lesser extent IL-1β, plays a role in restricting
196 rickettsiae survival. In agreement with our *in vivo* data, infection assays using BMDMΦ
197 also displayed an overall higher bacterial burden of both pathogenic *Rickettsia* spp., as
198 compared to the non-pathogenic *Rickettsia* strain (Figs. 4G and 1E). We further tested
199 the protein expression levels of pro-IL-1β and -IL-1α upon bacterial-infection of *WT*
200 BMDMΦ and showed that pro-IL-1β levels were induced by all three *Rickettsia* spp. to
201 similar levels (~5-fold) when compared to uninfected *WT* BMDMΦ (Fig. 4H). Intriguingly,
202 only *R. montanensis*-infected *WT* BMDMΦ produced significantly higher levels of pro-IL-
203 1α, as compared to *R. typhi*- or *R. rickettsii*-infected MΦ (Fig. 4H).
204

205 **Intracytosolic replication of pathogenic *Rickettsia* species in macrophages**
206 **depends on the inhibition of IL-1 cytokine secretion via a Caspase-11-Gsdmd-**
207 **dependent pathway.**

208 As our findings suggest that pathogenic, but not non-pathogenic, *Rickettsia* spp.
209 prevent the activation of signaling pathways required for IL-1α and IL-1β production and
210 release, we explored the mechanism of IL-1 signaling to a greater detail. As IL-1 signaling
211 responses commonly involves the canonical and non-canonical inflammasome pathways,
212 which in turn involves the proteolytic processing of both cytokines by activated Caspase
213 (Casp)-1 (canonical) and Casp-11 (non-canonical) respectively, we assessed their
214 potential role in regulating replication of non-pathogenic *vs*. pathogenic *Rickettsia* in
215 BMDMΦ. In this effort, BMDMΦ derived from *WT*, *Casp-1*$^{-/-}$, *Casp-11*$^{-/-}$, and *Casp-1/11*$^{-/-}$
216 mice were infected with *R. typhi*, *R. rickettsii*, and *R. montanensis* and the levels of IL-1β
217 and IL-1α, cell death, as well as bacterial burdens, were evaluated over the course of
218 infection. Our assays revealed that Casp-11 was involved in the secretion of cleaved IL-
219 1α upon infection of BMDMΦ with non-pathogenic and pathogenic *Rickettsia* spp. (Figs.
220 5A-B, D-E, and G-H). In addition, Casp-11-deficiency resulted in a significant decrease in
221 host cell death (Figs. 5C, F, and I). Casp-1-deficiency (*Casp-1*$^{-/-}$) caused a significant
222 decrease in IL-1β production [Figs. 5A, D, and G (green lines)], while IL-1α secretion as
223 well as the level of cell death remained unaffected during infection with all three *Rickettsia*
224 spp. [Figs. 5B-C, E-F, and H-I (green lines, symbols)]. Analysis of bacterial burdens
225 further revealed a prominent role for Casp-11, but not for Casp-1, in restricting the
226 replication of both pathogenic and non-pathogenic *Rickettsia* spp. (Fig. 5J; *WT* (square
227 symbols); *Casp-1*$^{-/-}$ (sphere symbols); *Casp-11*$^{-/-}$ (triangles symbols); *Casp-1/11*$^{-/-}$
228 (diamond symbols)]. As our findings indicate that infections with *R. typhi*- and *R. rickettsii*
229 resulted in a significant reduction of IL-1α secretion, likely via Casp-11-dependent
230 mechanism, we assessed the expression and activation status of Casp-1 and Casp-11

231 via Western blot analyses. *R. montanensis* infection resulted in a robust activation of
232 Casp-1, as indicative of the detection of the Casp-1-p20 fragment (Fig. 5K). In contrast,
233 infection with *R. typhi* and *R. rickettsii* spp. resulted in a lower activation of Casp-1 (~5-
234 fold) (Fig. 5K). Intriguingly, only infection with *R. montanensis* resulted in a robust
235 induction of Casp-11 (~8 fold) as compared to infection data using both pathogenic
236 *Rickettsia* spp. (Fig. 5K). To test if IL-1 cytokine secretion dependent on the bacterial load,
237 we heat-inactivated both pathogenic and non-pathogenic *Rickettsia* spp. and showed that
238 IL-1β and IL-1α release was significantly impaired as compared to infections using viable
239 *Rickettsia* spp., a phenotype more strongly observed in infections using *R. montanensis*
240 (Fig. S4). As IL-1 cytokine secretion dependents on Gsdmd, the pore-forming executor of
241 pyroptosis (29–32), we assessed the proteolytic processing of Gsdmd and showed that
242 only *R. montanensis* infection resulted in a robust cleavage of Gsdmd (~8 fold), as
243 indicative by the detection of the Gsdmd-p30 fragment (Fig. 5K). In support of our findings,
244 we showed that infection of *Gsdmd*$^{-/-}$ BMDMΦ with non-pathogenic and pathogenic
245 *Rickettsia* spp. released significantly lower levels of IL-1β and IL-1α, as compared to *WT*
246 BMDMΦ (Figs. S5A-B). Furthermore, analysis of bacterial burdens provided additional
247 evidence that Gsdmd plays a role in restricting the replication of *R. typhi*, *R. rickettsii*, and
248 *R. montanensis* (Fig. S5C). These findings suggest that pathogenic, unlike non-
249 pathogenic, *Rickettsia* spp. suppress IL-1 cytokine secretion via a Casp-11-Gsdmd-
250 dependent pathway to support an intracytosolic replication in MΦ.
251
252 **Secretion of IL-1α by macrophages is crucial in restricting the replication of**
253 **pathogenic and non-pathogenic *Rickettsia* species *in vivo*.**

254 To examine whether secretion of IL-1 by MΦ limits the replication of *Rickettsia* spp. *in*
255 *vivo*, we first injected (*i.v.*) *WT* mice with PBS- or dichloromethylene biphosphate
256 (Cl_2MBP)-liposomes to deplete endogenous macrophages as described previously [37].
257 Next, PBS- or Cl_2MBP-liposomes treated *WT* mice were injected (*i.v.*) with BMDMΦ
258 isolated from *WT*, *Il-1β*$^{-/-}$ or *Il-1α*$^{-/-}$ mice prior to infection with *R. typhi*, *R. rickettsii*, or *R.*
259 *montanensis*. Strikingly, adoptive transfer of *Il-1α*$^{-/-}$ BMDMΦ, but not *Il-1β*$^{-/-}$, or *WT* MΦ,
260 significantly increased the mortality of Cl_2MBP- but not PBS-treated *WT* mice injected
261 with all three *Rickettsia* spp., reaching levels similar to the survival percentages observed
262 in IL-1α Ab-neutralization studies (Figs. 6A-D, Fig. S6, and Fig. 2). Moreover, transfer of
263 *Il-1α*$^{-/-}$ BMDMΦ resulted in the development of splenomegaly (Fig. S7) and an increase in
264 bacterial burden in the spleens of Cl_2MBP-treated *WT* mice (Fig. 6E), which correlated
265 with a decrease in IL-1α serum concentrations without affecting IL-1β serum levels (Figs.
266 6F-G). In contrast, transfer of *Il-1β*$^{-/-}$ BMDMΦ, had an overall lesser effect on the severity
267 of rickettsiosis, as evidenced by a lower mortality rate, smaller spleen size, and lower
268 bacterial burden in Cl_2MBP-treated *WT* mice (Figs. 6A-E, and Fig. S7), which is in
269 agreement with our IL-1β Ab-neutralization data (Fig. 2). In addition, transfer of *Il-1β*$^{-/-}$
270 BMDMΦ, resulted in a decrease in IL-1β serum concentrations without affecting IL-1α
271 serum levels (Figs. 6F-G). Collectively, these data suggest that modulation of expression
272 and secretion of IL-1α secretion by macrophages is important to limit the replication of
273 *Rickettsia* spp. *in vivo*.
274
275 **Discussion**

276 Obligate intracellular bacterial pathogens, which successfully reside and replicate
277 within the host cell, overcome responses of innate immune defense surveillance (*e.g.*,
278 inflammasomes and autophagy). However, in the case of strict obligate intracytosolic
279 *Rickettsia* spp., the roles for both inflammasome and autophagy to restrict their replication
280 in endothelial cells and immune cells, like MΦ, is only now emerging, although without
281 consistent mechanistical insights (23–28, 33). Given these knowledge gaps and our
282 current lack of understanding on how TG *Rickettsia* spp. evade immune defense
283 responses to facilitate host colonization, we established an animal model of rickettsiosis
284 using C57BL/6J *WT* mice by comparing both mild (~LD_{25}) and more severe disease
285 (~LD_{50}) development for two pathogenic spp., *R. rickettsii*, and *R. typhi*. In fact, data of
286 disease severity correlated with the levels of bacterial burden detected in the mice
287 spleens. We also observed that infections with pathogenic, but not non-pathogenic,
288 *Rickettsia* spp. resulted in a reduced serum response of both pro-inflammatory cytokines,
289 IL-1β and IL-1α, which is likely the result of pathogenic *Rickettsia* spp. to evade canonical
290 and non-canonical inflammasome-dependent defense sensing, of which the former is in
291 agreement with recent studies using *R. australis* (26). Thus, our data suggests that
292 inhibition of both canonical and non-canonical inflammasome-dependent signaling
293 contributes to the enhanced survival and colonization of pathogenic *Rickettsia* spp. in our
294 *in vivo* experiments.

295 Our data further suggest that IL-1α, and to significantly lower extent IL-1β, plays a role
296 in limiting rickettsial infection *in vivo*. By testing the putative anti-rickettsial capabilities of
297 these cytokines through employing Ab-neutralization and recombinant protein assays, we
298 showed that IL-1α, and to a much lesser level IL-1β, was able to restrict the replication

299 and colonization of both non-pathogenic and pathogenic *Rickettsia* spp. *in vivo*. Our
300 current understanding by which *Rickettsia* spp. evade host-induced anti-bacterial
301 activities, and in particular, how cytosolic rickettsiae overcome host immune surveillance
302 in defense cells, like MΦ, is primarily based on reports that are not aligned with one
303 another (23–25, 27). Thus, we sought to address the hypothesis that pathogenic *R. typhi*,
304 and *R. rickettsii* spp. but not non-pathogenic *R. montanensis* evade innate immune
305 defense responses, in order, to establish an intracytosolic replication niche in MΦ. In
306 agreement with our *in vivo* infection models, *R. montanensis*-infected *WT* BMDMΦ
307 produced higher levels of IL-1α and IL-1β cytokines and displayed reduced bacterial loads
308 during the course of infection, compared to *R. typhi*- or *R. rickettsii*-infected BMDMΦ.
309 These data support the notion that non-pathogenic, but not pathogenic, *Rickettsia* spp.
310 are more efficiently cleared by MΦ, a mechanism that further supports the previously
311 published findings with SFG *Rickettsia* using THP-1 cells, a human macrophage-like cell
312 line (34). Collectively, our presented data strengthen our hypothesis that pathogenic, but
313 not non-pathogenic, *Rickettsia* spp. suppress anti-rickettsial inflammasome-dependent
314 IL-1 cytokine responses to establish an intracytosolic replication niche in MΦ.

315 Given that IL-1 signaling is modulated through inflammasome-dependent Casp-1,
316 Casp-11, and Gsdmd activation, we tested the role of both caspases as well as Gsdmd,
317 and found that non-pathogenic, but not pathogenic, *Rickettsia* spp. ensued Casp-1
318 activation and Casp-11 induction, which ultimately resulted in the proteolytic processing
319 of Gsdmd and release of IL-1α and IL-1β cytokines. Intriguingly, the lack of Casp-11
320 induction by pathogenic, but not non-pathogenic, *Rickettsia* spp. suggest that the
321 membrane-bound LPS of *R. typhi*, and *R. rickettsii* spp. is likely less immunogenic than

322 that of *R. montanensis*, which is further supported by our recent reports (35, 36). Our
323 findings further suggest that pathogenic, as compared to non-pathogenic, *Rickettsia* spp.,
324 benefit from evasion of the Casp-11-Gsdmd-IL-1α signaling axis to establish a replication
325 niche in MΦ as evidenced by the increased replication in MΦ from *Casp-11*$^{-/-}$, *Casp-1/11*$^{-}$
326 $^{/-}$, or *Gsdmd*$^{-/-}$ mice compared to *WT* and *Casp-1*$^{-/-}$ BMDMΦ. Finally, we sought to
327 determine the role of IL-1 cytokine responses by MΦ in restricting the replication of
328 *Rickettsia* spp. and showed that transfer of *Il-1α*$^{-/-}$ BMDMΦ, and to much lesser extent the
329 administration of *Il-1β*$^{-/-}$ BMDMΦ, exacerbated the disease progression in *WT* mice
330 injected with either pathogenic or non-pathogenic *Rickettsia* spp. It is worth noting that
331 the observed differences in IL-1α release could be partially attributed to alternative
332 mechanisms, including the retainment of IL-1α in the cytosol or nucleus, the dependance
333 of IL-1β, and/or the association with the decoy receptor of IL-1 (IL-1R2), and future
334 experiments are underway to address these possibilities (15, 29, 37–40). Also, IL-1α is
335 produced by other immune cells, such as neutrophils (15). Although our study did not
336 evaluate a potential contributing role of neutrophils, preceding findings suggest that
337 neutrophils did not alter the course of rickettsiosis or contribute to the restriction of
338 bacterial growth (28).

339 Importantly, preceding findings suggest that intracellular pathogens, like rickettsiae,
340 not only encounter inflammasome-dependent defense mechanisms but are also
341 confronted by another cytosolic defense pathway, autophagy (23, 25). Both responses
342 not only are key to mount the appropriate host defense responses (16, 18) but are also
343 functionally interconnected. In fact, recent reports indicated that autophagy acts on
344 intracellular microbes upstream of the inflammasome and thereby functions as a negative

345 regulator by degrading inflammasome components (10, 16, 18, 22). In the case of
346 rickettsiae, however, the role of autophagy in regulating inflammasome responses to
347 facilitate their host colonization remains inconclusive. For instance, *R. australis*, a
348 pathogenic TRG member, benefited from ATG5-dependent autophagy induction and
349 suppression of inflammasome-dependent IL-1β production to colonize MΦ (23, 25). In
350 contrast, *R. parkeri*, a mildly pathogenic member of SFG, demonstrated that its surface
351 protein OmpB is critical for protecting against autophagic recognition, while evasion of
352 autophagy was critical for invasion of BMDMΦ and *WT* mice by *R. parkeri* (24, 27).
353 Intriguingly, our recent report on *R. typhi* showed that *R. typhi* is ubiquitinated upon host
354 entry, induces autophagy, but escapes autophagolysosomal maturation for intracellular
355 colonization in non-phagocytic cells (9). Given these reports by others and our recent
356 findings, it is tempting to speculate that pathogenic, but not non-pathogenic, *Rickettsia*
357 spp. induce autophagy to down-regulate inflammasome-dependent IL-1β and IL-1α
358 cytokine responses to establish an intracytosolic replication niche *in vitro* and *in vivo*, and
359 our future research will address this possibility.

360 Overall, our findings present a previously unappreciated model of host invasion by
361 which pathogenic, but not non-pathogenic, *Rickettsia* spp., avoid the activation of
362 signaling pathways required for IL-1α production and release; likely via the suppression
363 of the Casp-11-Gsdmd signaling pathway, to facilitate their intracytosolic replication in
364 MΦ and ultimately cause host colonization (Fig. 6H).

365

366 **Materials and Methods**

367 **Animals**

368 All experiments were conducted in fully AAALAC accredited program using 8-10 weeks
369 old female C57BL/6J *WT* mice in a specific pathogen-free environment according to the
370 University of Maryland School of Medicine Institutional Animal Care and Use Committee
371 (IACUC) in compliance with the National Institutes of Health Guide.
372
373 **Antibodies and reagents**
374 Anti(α)-IL-1α (clone ALF-161), αIL-1β (clone B122), or an isotype control IgG (Armenian
375 hamster IgG) antibody (Ab) were purchased from BioXCell. αCaspase (Casp)-1 Ab was
376 purchased from Adipogen, while αCasp-11 [EPR18628] and αGsdmd [EPR19828] Abs
377 were obtained from Abcam. Elongation factor Ts (EF-Ts) Ab was obtained from Primm
378 Biotech as previously described (9), while the αGapdh (FL-335) Ab was purchased from
379 Santa Cruz Biotechnology. Halt protease and phosphatase inhibitor cocktail was obtained
380 from Thermo Fisher Scientific. Endotoxin-free recombinant mouse IL-1α and IL-1β
381 proteins were purchased from BioLegend.
382
383 **Bacterial strains, cell culture, and infection**
384 Vero76 cells (African green monkey kidney, ATCC, RL-1587) were maintained in minimal
385 Dulbecco's modified Eagle's medium (DMEM) supplemented with 10% heat-inactivated
386 fetal bovine serum (FBS) at 37°C with 5% CO_2. *R. montanensis* strain M5/6 and *R.*
387 *rickettsia* strain Sheila Smith (*SS*) were obtained from Dr. Ted Hackstadt (Rocky Mountain
388 Laboratories, NIH, MT, USA) and *R. typhi* strain Wilmington was obtained from CDC. All
389 *Rickettsia* strains were propagated in Vero76 cells grown in DMEM supplemented with
390 5% FBS at 34°C with 5% CO_2. All *Rickettsia* were purified as previously described (7).

391 For infection of BMDMΦ, purified *Rickettsia* spp. were used at a multiplicity of infection
392 (MOI) of 50, to ensure the presence of enough bacteria at early stage of infection, for host
393 response (5, 8, 9). For infection using heat-inactivated bacteria, purified *Rickettsia* spp.
394 were heated at 90ºC for 20 min (41). Rickettsiosis in mice was induced by tail vein
395 injection (*i.v.*) of purified *Rickettsia* (10^5-10^6 PFU), resuspended in PBS. At Days 1, 3, and
396 7 after administration, blood was collected, and serum cytokine levels were measured by
397 flow cytometry. Splenic tissue specimens were collected at the indicated times and used
398 for bacterial burden analysis by qPCR described below.
399

400 **Differentiation of bone marrow-derived macrophages**

401 Bone marrow cells were isolated from femurs and tibias of *WT*, *Il-1β*$^{-/-}$ or *Il-1α*$^{-/-}$, *Gsdmd*$^{-/-}$
402 , *Casp-1*$^{-/-}$, *Casp-11*$^{-/-}$, *Casp-1/Casp-11*$^{-/-}$ mice. Femurs from *Casp-1*$^{-/-}$, *Casp-11*$^{-/-}$, *Casp-*
403 *1/Casp-11*$^{-/-}$ were kindly provided by Dr. Amal Amer (The Ohio State University, OH,
404 USA), while bones from *Il-1β*$^{-/-}$ or *Il-1α*$^{-/-}$ mice were obtained from Dr. Thirumala-Devi
405 Kanneganti (St. Jude Children's Research Hospital, TN, USA). Femurs from *Gsdmd*$^{-/-}$
406 were kindly provided by Dr. Matthew Welch (University of California, Berkeley, CA, USA).
407 Differentiation was induced by culturing bone marrow cells in RPMI 1640 medium
408 supplemented with 10% FBS and 30% L929-conditioned medium (a source of
409 macrophage colony stimulating factor) and cultured for 7 days as described previously
410 (42).
411

412 **Measurement of cytokines and chemokines**

413 IL-1 cytokine concentrations in the sera of mice or supernatants from cultured BMDMΦ
414 were assessed using the Legendplex mouse inflammation kit (BioLegend) following the
415 manufacturer's instructions as described previously (42).
416
417 **RNA isolation and quantitative real-time PCR**
418 BMDMΦ samples were collected at 2, 6, 24, and 48 h post-infection, while spleens were
419 collected at day 3 or 7 post infection. RNA was extracted from 1 x 10^6 BMDMΦ or 100 µl
420 of organ homogenate using the Quick-RNA miniprep kit (ZymoResearch). The iScript
421 Reverse Transcription Supermix kit (Bio-Rad; 1708841) was used to synthesize cDNAs
422 from 200 ng of RNA according to the manufacturer's instructions. Quantitative real-time
423 PCR was performed using SYBR Green (Thermo Fisher Scientific), 2 µl cDNA and 1 µM
424 each of the following oligonucleotides for rickettsial citrate synthase gene (*gltA*) forward
425 (F): 5'-CATAATAGCCATAGGATGAG-3'; reverse (R): 5'-ATGATTTATGGGGAACTACC-
426 3' and analyzed as described previously (25). Oligonucleotides for *Gapdh* were obtained
427 from Qiagen.
428
429 **Extract preparation, and Western blot analysis.**
430 *Rickettsia*-infected BMDMΦ cells were lysed for 2 h at 4°C in ice-cold lysis buffer (50 mM
431 HEPES [pH 7.4], 137 mM NaCl, 10% glycerol, 1 mM EDTA, 0.5% NP-40, and
432 supplemented with protease and phosphatase inhibitory cocktails) as described
433 previously (42). Equal amounts of protein were loaded for SDS-PAGE and membranes
434 were probed with αCasp-1, αCasp-11, αGsdmd, αIL-1α, αIL-1β, αEF-Ts, and αGapdh

435 Abs, followed by enhanced chemiluminescence with secondary Abs conjugated to
436 horseradish peroxidase.
437
438 **Neutralization of endogenous IL-1α and IL-1β**
439 For *in vivo* neutralization of IL-1α and IL-1β, C57BL/6J *WT* mice were *i.v.* injected with
440 250 mg of αIL-1α (clone ALF-161, BioXCell), αIL-1β (clone B122, BioXCell), or an IgG-
441 isotype control (Armenian hamster IgG, BioXCell) Ab 24 h before the induction of mild
442 rickettsiosis using 10^5 PFU of *R. typhi*, *R. rickettsii*, or *R. montanensis*.
443
444 **Adoptive transfer of bone marrow-derived macrophages**
445 C57BL/6J *WT* mice were injected (*i.v.*) twice with PBS- or dichloromethylene biphosphate
446 (Cl_2MBP)-liposomes 72 and 48 hours prior to macrophage transfer as described
447 previously (42). Next, C57BL/6J *WT* mice were injected (*i.v.*) with *WT*, *Il-1β*$^{-/-}$ or *Il-1α*$^{-/-}$
448 BMDMΦ [5 x 10^6 cells/mouse] followed by infection (24 hours post-MΦ transfer) with *R.*
449 *typhi*, *R. rickettsii*, *R. montanensis*, or PBS (dose 10^5 PFU).
450
451 **Statistical analysis**
452 Endpoint studies of mice subjected to mild (10^5 PFU) and severe (10^6 PFU) rickettsiosis
453 were analyzed by using Kaplan-Meir survival curves and the log-rank test (GraphPad
454 Prism Software, version 8). The statistical significance was assessed using ANOVA with
455 Tukey's multiple comparisons post-test (GraphPad). Data are presented as mean ± SEM,
456 unless stated otherwise. Alpha level was set to 0.05.
457

Acknowledgments

We gratefully acknowledge Drs. Amal Amer (The Ohio State University, OH, USA), Thirumala-Devi Kanneganti (St. Jude Children's Research Hospital, TN, USA), Matthew Welch (University of California, Berkeley, CA, USA) and Ted Hackstadt (Rocky Mountain Laboratories, NIH, MT, USA) for generously providing us with essential biological specimens and reagents, including femurs from various knock-out mice and rickettsial strains. We would like to thank Magda Beier-Sexton for her administrative, technical, organizational, and editorial contributions as well as Dr. Stefanie Vogel (University of Maryland School of Medicine, Baltimore, MD, USA) for critical discussions and editorial contributions to the manuscript. This work was supported with funds from the NIAID/NIH grants (R01AI017828 and R01AI126853 to A.F.A.).

Conflicts of Interest

The authors declare no conflict of interest. The funding sources had no role in the design of the study, in the collection, analyses, or interpretation of data, in the writing of the manuscript, or in the decision to publish the results.

References

1. Ray K, Marteyn B, Sansonetti PJ, Tang CM. 2009. Life on the inside: the intracellular lifestyle of cytosolic bacteria. Nat Rev Microbiol 7:333–340.
2. Personnic N, Bärlocher K, Finsel I, Hilbi H. 2016. Subversion of Retrograde Trafficking by Translocated Pathogen Effectors. Trends Microbiol 24:450–462.
3. Sahni A, Fang R, Sahni SK, Walker DH. 2019. Pathogenesis of Rickettsial Diseases: Pathogenic and Immune Mechanisms of an Endotheliotropic Infection. Annu Rev Pathol 14:127–152.
4. Lehman SS, Noriea NF, Aistleitner K, Clark TR, Dooley CA, Nair V, Kaur SJ, Rahman MS, Gillespie JJ, Azad AF, Hackstadt T. 2018. The rickettsial ankyrin

485 repeat protein 2 is a type IV secreted effector that associates with the
486 endoplasmic reticulum. MBio 9.

487 5. Rahman MS, Ammerman NC, Sears KT, Ceraul SM, Azad AF. 2010. Functional
488 characterization of a phospholipase A(2) homolog from Rickettsia typhi. J
489 Bacteriol 192:3294–3303.

490 6. Rahman MS, Gillespie JJ, Kaur SJ, Sears KT, Ceraul SM, Beier-Sexton M, Azad
491 AF. 2013. Rickettsia typhi Possesses Phospholipase A2 Enzymes that Are
492 Involved in Infection of Host Cells. PLoS Pathog2013/07/03. 9:e1003399.

493 7. Rennoll-Bankert KE, Rahman MS, Gillespie JJ, Guillotte ML, Kaur SJ, Lehman
494 SS, Beier-Sexton M, Azad AF. 2015. Which Way In? The RalF Arf-GEF
495 Orchestrates Rickettsia Host Cell Invasion. PLoS Pathog 11:e1005115.

496 8. Rennoll-Bankert KE, Rahman MS, Guillotte ML, Lehman SS, Beier-Sexton M,
497 Gillespie JJ, Azad AF. 2016. RalF-Mediated Activation of Arf6 Controls Rickettsia
498 typhi Invasion by Co-Opting Phosphoinositol Metabolism. Infect Immun 84:3496–
499 3506.

500 9. Voss OH, Gillespie JJ, Lehman SS, Rennoll SA, Beier-Sexton M, Rahman MS,
501 Azad AF. 2020. Risk1, a Phosphatidylinositol 3-Kinase Effector, Promotes
502 Rickettsia typhi Intracellular Survival. MBio 11.

503 10. Sun Q, Fan J, Billiar TR, Scott MJ. 2017. Inflammasome and Autophagy
504 Regulation: A Two-way Street. Mol Med 23:188–195.

505 11. Place DE, Kanneganti TD. 2018. Recent advances in inflammasome biology. Curr
506 Opin Immunol. Elsevier Ltd.

507 12. Xue Y, Enosi Tuipulotu D, Tan WH, Kay C, Man SM. 2019. Emerging Activators
508 and Regulators of Inflammasomes and Pyroptosis. Trends Immunol. Elsevier Ltd.

509 13. Wiggins KA, Parry AJ, Cassidy LD, Humphry M, Webster SJ, Goodall JC, Narita
510 M, Clarke MCH. 2019. IL-1α cleavage by inflammatory caspases of the
511 noncanonical inflammasome controls the senescence-associated secretory
512 phenotype. Aging Cell 18:1–13.

513 14. Tapia VS, Daniels MJD, Palazón-Riquelme P, Dewhurst M, Luheshi NM, Rivers-
514 Auty J, Green J, Redondo-Castro E, Kaldis P, Lopez-Castejon G, Brough D.
515 2019. The three cytokines IL-1β, IL-18, and IL-1α share related but distinct
516 secretory routes. J Biol Chem 294:8325–8335.

517 15. Malik A, Kanneganti T-D. 2018. Function and regulation of IL-1α in inflammatory
518 diseases and cancer. Immunol Rev 281:124–137.

519 16. Krakauer T. 2019. Inflammasomes, Autophagy, and Cell Death: The Trinity of
520 Innate Host Defense against Intracellular Bacteria. Mediators Inflamm 2019:1–10.

521 17. Mitchell G, Isberg RR. 2017. Innate Immunity to Intracellular Pathogens:
522 Balancing Microbial Elimination and Inflammation. Cell Host Microbe.

523 18. Seveau S, Turner J, Gavrilin MA, Torrelles JB, Hall-Stoodley L, Yount JS, Amer

524 AO. 2018. Checks and Balances between Autophagy and Inflammasomes during
525 Infection. J Mol Biol 430:174–192.

526 19. Storek KM, Monack DM. 2015. Bacterial recognition pathways that lead to
527 inflammasome activation. Immunol Rev.

528 20. Vladimer GI, Marty-Roix R, Ghosh S, Weng D, Lien E. 2013. Inflammasomes and
529 host defenses against bacterial infections. Curr Opin Microbiol.

530 21. Zheng D, Liwinski T, Elinav E. 2020. Inflammasome activation and regulation:
531 toward a better understanding of complex mechanisms. Cell Discov 6:36.

532 22. Takahama M, Akira S, Saitoh T. 2018. Autophagy limits activation of the
533 inflammasomes. Immunol Rev. Blackwell Publishing Ltd.

534 23. Bechelli J, Vergara L, Smalley C, Buzhdygan TP, Bender S, Zhang W, Liu Y,
535 Popov VL, Wang J, Garg N, Hwang S, Walker DH, Fang R. 2019. Atg5 supports
536 Rickettsia australis infection in macrophages in vitro and in vivo. Infect Immun 87.

537 24. Burke TP, Engström P, Chavez RA, Fonbuena JA, Vance RE, Welch MD. 2020.
538 Inflammasome-mediated antagonism of type I interferon enhances Rickettsia
539 pathogenesis. Nat Microbiol 5:688–696.

540 25. Smalley C, Bechelli J, Rockx-Brouwer D, Saito T, Azar SR, Ismail N, Walker DH,
541 Fang R. 2016. Rickettsia australis Activates Inflammasome in Human and Murine
542 Macrophages. PLoS One 11:e0157231.

543 26. Rumfield C, Hyseni I, McBride JW, Walker DH, Fang R. 2020. Activation of ASC
544 inflammasome driven by toll-like receptor 4 contributes to host immunity against
545 rickettsial infection. Infect Immun 88.

546 27. Engström P, Burke TP, Mitchell G, Ingabire N, Mark KG, Golovkine G, Iavarone
547 AT, Rape M, Cox JS, Welch MD. 2019. Evasion of autophagy mediated by
548 Rickettsia surface protein OmpB is critical for virulence. Nat Microbiol 4:2538–
549 2551.

550 28. Papp S, Moderzynski K, Rauch J, Heine L, Kuehl S, Richardt U, Mueller H,
551 Fleischer B, Osterloh A. 2016. Liver Necrosis and Lethal Systemic Inflammation in
552 a Murine Model of Rickettsia typhi Infection: Role of Neutrophils, Macrophages
553 and NK Cells. PLoS Negl Trop Dis 10:e0004935.

554 29. Batista SJ, Still KM, Johanson D, Thompson JA, O'Brien CA, Lukens JR, Harris
555 TH. 2020. Gasdermin-D-dependent IL-1α release from microglia promotes
556 protective immunity during chronic Toxoplasma gondii infection. Nat Commun
557 11:1–13.

558 30. Kanneganti A, Malireddi RKS, Saavedra PHV, Walle L Vande, Van Gorp H,
559 Kambara H, Tillman H, Vogel P, Luo HR, Xavier RJ, Chi H, Lamkanfi M. 2018.
560 GSD MD is critical for autoinflammatory pathology in a mouse model of Familial
561 Mediterranean Fever. J Exp Med 215:1519–1529.

562 31. Liu X, Zhang Z, Ruan J, Pan Y, Magupalli VG, Wu H, Lieberman J. 2016.
563 Inflammasome-activated gasdermin D causes pyroptosis by forming membrane

564 pores. Nature 535:153–158.

565 32. Tsuchiya K, Hosojima S, Hara H, Kushiyama H, Mahib MR, Kinoshita T, Suda T.
566 2021. Gasdermin D mediates the maturation and release of IL-1α downstream of
567 inflammasomes. Cell Rep 34:108887.

568 33. Moderzynski K, Papp S, Rauch J, Heine L, Kuehl S, Richardt U, Fleischer B,
569 Osterloh A. 2016. CD4+T Cells Are as Protective as CD8+T Cells against
570 Rickettsia typhi Infection by Activating Macrophage Bactericidal Activity. PLoS
571 Negl Trop Dis 10.

572 34. Curto P, Simões I, Riley SP, Martinez JJ. 2016. Differences in intracellular fate of
573 two spotted fever group Rickettsia in macrophage-like cells. Front Cell Infect
574 Microbiol 6.

575 35. Guillotte ML, Gillespie JJ, Chandler CE, Rahman MS, Ernst RK, Azad AF. 2018.
576 Rickettsia lipid A biosynthesis utilizes the late acyltransferase LpxJ for secondary
577 fatty acid addition. J Bacteriol 200.

578 36. Guillotte ML, Chandler CE, Verhoeve VI, Gillespie JJ, Driscoll TP, Rahman MS,
579 Ernst RK, Azad AF. 2021. Lipid A Structural Divergence in Rickettsia Pathogens.
580 mSphere 6.

581 37. Fettelschoss A, Kistowska M, LeibundGut-Landmann S, Beer H-D, Johansen P,
582 Senti G, Contassot E, Bachmann MF, French LE, Oxenius A, Kündig TM. 2011.
583 Inflammasome activation and IL-1β target IL-1α for secretion as opposed to
584 surface expression. Proc Natl Acad Sci U S A 108:18055.

585 38. Paolo NC Di, Shayakhmetov DM. 2016. Interleukin 1α and the inflammatory
586 process. Nat Immunol 17:906.

587 39. Peters VA, Joesting JJ, Freund GG. 2013. IL-1 receptor 2 (IL-1R2) and its role in
588 immune regulation. Brain Behav Immun 32:1.

589 40. Shi L, Song L, Maurer K, Dou Y, Patel VR, Su C, Leonard ME, Lu S, Hodge KM,
590 Torres A, Chesi A, Grant SFA, Wells AD, Zhang Z, Petri MA, Sullivan KE. 2020.
591 IL-1 Transcriptional Responses to Lipopolysaccharides Are Regulated by a
592 Complex of RNA Binding Proteins. J Immunol 204:1334–1344.

593 41. Ammerman NC, Beier-Sexton M, Azad AF. 2008. Laboratory Maintenance of
594 Rickettsia rickettsii. Curr Protoc Microbiol Chapter 3:Unit 3A.5.

595 42. Voss OH, Murakami Y, Pena MY, Lee H-N, Tian L, Margulies DH, Street JM,
596 Yuen PST, Qi C-F, Krzewski K, Coligan JE. 2016. Lipopolysaccharide-Induced
597 CD300b Receptor Binding to Toll-like Receptor 4 Alters Signaling to Drive
598 Cytokine Responses that Enhance Septic Shock. Immunity 44:1365–1378.

599 43. Voss OH, Arango D, Tossey JC, Villalona Calero MA, Doseff AI. 2021. Splicing
600 reprogramming of TRAIL/DISC-components sensitizes lung cancer cells to
601 TRAIL-mediated apoptosis. Cell Death Dis 12.

602

603 **Figure Legend**

604 **Fig. 1 *In vivo* models of rickettsiosis.**

605 (**A**) *Rickettsia* spp. and their level of pathogenicity to humans (3, 43).

606 (**B-D**) Establishment of a model of rickettsiosis (LD_{25} and LD_{50}) for *R. typhi* [B], *R. rickettsii*

607 [C] or *R. montanensis* [D] in C57BL/6J *WT* mice. Animals were injected via tail vein (*i.v.*)

608 with different doses [10^5-10^6 PFU] of *R. typhi*, *R. rickettsii*, *R. montanensis*, or PBS (n=12

609 for each treatment). Survival was monitored for 7 days.

610 (**E**) Bacterial burden was tested in spleens of *R. typhi*-, *R. rickettsii*-, *R. montanensis*-, or

611 PBS-injected *WT* mice (n=5 per each treatment) shown in (B-D) by *GltA* RT-qPCR at day

612 3 and 7 (n=5 for each treatment) using the host housekeeping gene, *Gapdh*, for

613 normalization.

614 (**F-G**) Serum samples from rickettsiae-infected mice described in (B-D) were analyzed for

615 IL-1β (F) and IL-1α (G) production using the Legendplex kits (BioLegend) followed by flow

616 cytometry analysis.

617 Error bars in (E-G) represent means ± SEM from five independent experiments; NS, non-

618 significant; *$p \leq 0.05$; **$p \leq 0.01$; ***$p \leq 0.005$; ****$p \leq 0.001$.

619

620 **Fig. 2 Neutralization of IL-1α activity augments mortality of pathogenic and non-**

621 **pathogenic *Rickettsia*-induced rickettsiosis.**

622 (**A-C**) C57BL/6J *WT* mice were injected via tail vein (*i.v.*) with 10^5 PFU of *R. typhi* [A], *R.*

623 *rickettsii* [B], or *R. montanensis* [C] (A-C; n=12 for each treatment) followed by a

624 subsequent injection (*i.v.*) with αIL-1β, αIL-1α or IgG-isotype control antibody (Ab) [250

625 μg Ab/mouse]. Survival was monitored for 7 days.

626 (**D**) Bacterial burden was tested in spleens of Ab-treated *R. typhi*-, *R. rickettsii*-, and *R.*
627 *montanensis*-injected *WT* mice shown in (A-C) by *GltA* RT-qPCR at day 7 (n=5 for each
628 treatment) using the host housekeeping gene, *Gapdh*, for normalization.
629 (**E-F**) Serum samples from mice described in (A-C) were analyzed for IL-1β (E) and IL-
630 1α (F) production at day 7 (n=5 for each treatment) using the Legendplex kits (BioLegend)
631 followed by flow cytometry analysis.
632 Error bars in (D-F) represent means ± SEM from five independent experiments; NS, non-
633 significant; *$p \leq 0.05$; **$p \leq 0.01$; ***$p \leq 0.005$; ****$p \leq 0.001$.
634
635 **Fig. 3 Administration of recombinant IL-1α rescues fatal *Rickettsia*-induced**
636 **rickettsiosis.**
637 (**A-C**) C57BL/6J *WT* mice were injected *i.v.* with recombinant (r)IL-1β or rIL-1α protein
638 [500 ng/mouse] followed by infection (24 h post protein injection) with 10^6 PFU of *R. typhi*
639 [A], *R. rickettsii* [B], *R. montanensis* [C], or PBS (A-C; n=15 for each treatment). Survival
640 was monitored for 7 days.
641 (**D**) Bacterial burden was tested in spleens of protein-treated *R. typhi*-, *R. rickettsii*-, *R.*
642 *montanensis*- or PBS-injected *WT* mice shown in (A-C) by *GltA* RT-qPCR at day 7 (n=5
643 for each treatment) using the housekeeping gene, *Gapdh*, for normalization.
644 (**E-F**) Serum samples from mice described in (A-C) were analyzed for IL-1β (E) and IL-
645 1α (F) production at day 7 (n=5 for each treatment) using the Legendplex kits (BioLegend)
646 followed by flow cytometry analysis.
647 Error bars in (D-F) represent means ± SEM from five independent experiments; NS, non-
648 significant; *$p \leq 0.05$; **$p \leq 0.01$; ***$p \leq 0.005$; ****$p \leq 0.001$.

649

650 **Fig. 4 IL-1α, but not IL-1β, contributes to the survival of *Rickettsia* species in**
651 **macrophages.**

652 (**A**-**F**) BMDMΦ from *WT*, *Il-1β*$^{-/-}$ or *Il-1α*$^{-/-}$ mice were infected with *R. typhi*, *R. rickettsii*, or
653 *R. montanensis* [MOI=50] for 0, 6, 24, and 48 h. Culture supernatants were analyzed for
654 production of IL-1β (A, C, and E) and IL-1α (B, D, and F) using Legendplex kits
655 (BioLegend) followed by flow cytometry.

656 (**G**) Bacterial burden in rickettsiae-infected BMDMΦ from *WT*, *Il-1β*$^{-/-}$ or *Il-1α*$^{-/-}$ mice was
657 evaluated at 2 and 24 h post-infection by *GltA* RT-qPCR. Expression of the housekeeping
658 gene *Gapdh* was used for normalization.

659 (**H**) BMDMΦ from *WT* mice were either left uninfected (-) or infected with *R. typhi*, *R.*
660 *rickettsii*, or *R. montanensis*, [MOI=50] for 24 h. Lysates were immunoblotted with αIL-1α,
661 αIL-1β, αET-Ts, and αGapdh Abs. Densitometry was performed using Fiji software and
662 data represent the fold-change ratios of pro-IL-1β/Gapdh or pro-IL-1α/Gapdh between
663 uninfected and infected cells are shown. Immunoblot data are a representative of three
664 independent experiments.

665 Error bars in (A-G) represent means ± SEM from five independent experiments; NS: non-
666 significant; *$p \leq 0.05$; **$p \leq 0.01$; ***$p \leq 0.005$; ****$p \leq 0.001$.

667

668 **Fig. 5 Pathogenic, but not non-pathogenic, *Rickettsia* species limit Caspase-1- and**
669 **Caspase-11-dependent IL-1 signaling to facilitate their intracellular replication in**
670 **macrophages.**

671 (**A-I**) BMDMΦ from *WT*, *Casp-1*$^{-/-}$, *Casp-11*$^{-/-}$, or *Casp-1/11*$^{-/-}$ mice were infected with *R.*
672 *typhi* (A-C), *R. rickettsii* (D-F) or *R. montanensis* (G-I) [MOI=50] for 0, 6, 24, and 48 h.
673 Culture supernatants were analyzed for production of IL-1β (A, D, G) and IL-1α (B, E, H)
674 using Legendplex kits (BioLegend) followed by flow cytometry. BMDM cell death at 24 h
675 post-infection, was measured by LDH release assay (C, F, I).
676 (**J**) Bacterial burdens in infected BMDMΦ were evaluated 2 and 24 h post-infection by
677 *GltA* RT-qPCR. Expression of the host housekeeping gene *Gapdh* was used for
678 normalization.
679 (**K**) Western analysis of Casp-1, Casp-11, and Gsdmd induction and processing at 24 h
680 post-infection with *R. typhi*, *R. rickettsii*, or *R. montanensis* using αCasp-1, αCasp-11, and
681 αGsdmd Abs. Reblotting with rickettsial specific αEF-Ts and host cell specific αGapdh
682 Abs served as infection and equal loading controls respectively. Densitometry was
683 performed using Fiji software and data represent the fold-change ratios of Casp-1-p20/
684 FL-Casp-1; Gsdmd-p30/FL-Gsdmd; or Casp-11/Gapdh between uninfected and infected
685 cells are shown.
686 Error bars in (A-J) represent means ± SEM from five independent experiments; NS: non-
687 significant; *$p \leq 0.05$; **$p \leq 0.01$; ***$p \leq 0.005$; ****$p \leq 0.001$. Immunoblot data are a
688 representative of three independent experiments.
689
690 **Fig. 6 Macrophages-dependent secretion of IL-1α contributes more than IL-1β for**
691 **controlling the survival and colonization of pathogenic and non-pathogenic**
692 ***Rickettsia* species.**

693 (**A-D**) Dichloromethylene biphosphate (Cl_2MBP)-treated C57BL/6J *WT* mice were
694 injected *i.v.* with *WT*, *Il-1β*$^{-/-}$ or *Il-1α*$^{-/-}$ BMDMΦ [5 x 10^6 cells/mouse] followed by infection
695 (24 h post-MΦ transfer) with *R. typhi* [B], *R. rickettsii* [C], or *R. montanensis* [D] (dose 10^5
696 PFU) (B-D; n=12 for each treatment). Survival was monitored for 7 days.
697 (**E**) Bacterial burden was tested in spleens from mice described in (B-D) by *GltA* RT-
698 qPCR at day 7 (n=5 for each treatment) using the housekeeping gene, *Gapdh*, for
699 normalization.
700 (**F-G**) Serum samples from mice described in (B-D) were analyzed for IL-1β (F) and IL-
701 1α (G) production at day 7 (n=5 for each treatment) using the Legendplex kits (BioLegend)
702 followed by flow cytometry analysis.
703 Error bars in (E-G) represent means ± SEM from five independent experiments; NS, non-
704 significant; *$p \leq 0.05$; **$p \leq 0.01$; ***$p \leq 0.005$; ****$p \leq 0.001$.
705 (**H**) Proposed working model on how pathogenic *Rickettsia* spp. suppress Casp-1 and
706 Casp-11-dependent IL-1 signaling responses to establish a replication niche *in vitro* and
707 *in vivo*. Of note, the majority of non-pathogenic *Rickettsia* spp. is likely destroyed by
708 phagolysosomal fusion, while a subpopulation may escape lysosomal fusion, ultimately
709 allowing for the induction of inflammasome mediated IL-1 responses.
710
711 **Fig. S1. Splenic data during infection of pathogenic and non-pathogenic *Rickettsia***
712 **species.**
713 (**A**) Representative images of spleens (at day 7) from C57BL/6J *WT* mice injected *i.v.*
714 with *R. typhi*, *R. rickettsii*, *R. montanensis*, or PBS (dose 10^6 PFU).
715 (**B**) Spleen weight from injected animals was evaluated at day 7 day (n=5).

716 Error bars in (B) represent means ± SEM from five independent experiments; *$p \leq 0.05$;
717 ***$p \leq 0.005$.
718
719 **Fig. S2. Splenic data after IL-1 signaling neutralization during infection of**
720 **pathogenic and non-pathogenic *Rickettsia* species.**
721 (**A**) Representative images of spleens (day 7) from C57BL/6J *WT* mice injected *i.v.* with
722 *R. typhi*, *R. rickettsii*, or *R. montanensis* (dose 10^5 PFU) followed by administration of αIL-
723 1β, αIL-1α, or IgG isotype control antibody (Ab) [250 μg Ab/mouse] (24 h post-Ab
724 injection).
725 (**B**) Spleen weight from injected animals was evaluated at day 7 (n=5).
726 Error bars in (B) represent means ± SEM from five independent experiments; *$p \leq 0.05$;
727 **$p \leq 0.01$; ***$p \leq 0.005$.
728
729 **Fig. S3 Splenic data after administration of recombinant IL-1α and IL-1β proteins**
730 **during infection of pathogenic and non-pathogenic *Rickettsia* species.**
731 (**A**) Representative images of spleens (day 7) from C57BL/6J *WT* mice injected *i.v.* with
732 rIL-1β or rIL-1α protein followed by administration of *R. typhi*, *R. rickettsii*, *R. montanensis*
733 or PBS (dose 10^6 PFU) at day 7.
734 (**B**) Spleen weight from injected animals was evaluated at day 7 day (n=5).
735 Error bars in (B) represent means ± SEM from five independent experiments; *$p \leq 0.05$;
736 **$p \leq 0.01$; ***$p \leq 0.005$.
737

738 **Fig. S4 Heat-inactivation of *Rickettsia* species resulted in a reduced IL-1α and IL-**
739 **1β cytokine release by macrophages.**
740 (**A-B**) BMDMΦ from *WT* mice were infected with heat-inactivated or non-heat treated *R.*
741 *typhi*, *R. rickettsii*, or *R. montanensis* [MOI=50] for 24 h. Culture supernatants were
742 analyzed for production of IL-1β (A) and IL-1α (B) using Legendplex kits (BioLegend)
743 followed by flow cytometry.
744 (**C**) Bacterial burden in rickettsiae-infected BMDMΦ from *WT* mice was evaluated at 2
745 and 24 h post-infection by *GltA* RT-qPCR. Expression of the housekeeping gene *Gapdh*
746 was used for normalization.
747 Error bars in (A-C) represent means ± SEM from five independent experiments; NS: non-
748 significant; ****p* ≤ 0.01; *****p* ≤ 0.005; ******p* ≤ 0.001.
749
750 **Fig. S5 Gsdmd is involved in the release of IL-1α and IL-1β by macrophages upon**
751 ***Rickettsia* infection.**
752 (**A-B**) BMDMΦ from *WT* and *Gsdmd*$^{-/-}$ mice were infected with *R. typhi*, *R. rickettsii*, or *R.*
753 *montanensis* [MOI=50] for 24 h. Culture supernatants were analyzed for production of IL-
754 1β (A) and IL-1α (B) using Legendplex kits (BioLegend) followed by flow cytometry.
755 (**C**) Bacterial burden in rickettsiae-infected BMDMΦ from *WT* and *Gsdmd*$^{-/-}$ mice was
756 evaluated at 2 and 24 h post-infection by *GltA* RT-qPCR. Expression of the housekeeping
757 gene *Gapdh* was used for normalization.
758 Error bars in (A-C) represent means ± SEM from five independent experiments; NS: non-
759 significant; **p* ≤ 0.05; ****p* ≤ 0.01; *****p* ≤ 0.005.
760

761 **Fig. S6 Survival data after adoptive transfer of *WT*, *Il-1β*$^{-/-}$ or *Il-1α*$^{-/-}$ macrophages**
762 **and infection of pathogenic and non-pathogenic *Rickettsia* species into PBS-**
763 **liposome-treated C57BL/6J *WT* mice.** (A-D) PBS-treated C57BL/6J *WT* mice were
764 injected *i.v.* with *WT*, *Il-1β*$^{-/-}$ or *Il-1α*$^{-/-}$ BMDMΦ [5 x 10^6 cells/mouse] followed by infection
765 (24 h post-MΦ transfer) with *R. typhi* [B], *R. rickettsii* [C], *R. montanensis* [D], or PBS
766 (dose 10^5 PFU) (B-D; n=12 for each treatment). Survival was monitored for 7 days.
767
768 **Fig. S7. Splenic data after adoptive transfer of *WT*, *Il-1β*$^{-/-}$ or *Il-1α*$^{-/-}$ macrophages**
769 **and infection of pathogenic and non-pathogenic *Rickettsia* species into**
770 **dichloromethylene biphosphate (Cl_2MBP)-treated C57BL/6J *WT* mice.**
771 (**A**) Representative images of spleens (day 7) from Cl_2MBP-treated C57BL/6J *WT* mice
772 injected *i.v.* with *WT*, *Il-1β*$^{-/-}$ or *Il-1α*$^{-/-}$ BMDMΦ [5 x 10^6 cells/mouse] followed by
773 administration (24 h post-MΦ transfer) of *R. typhi*, *R. rickettsii*, *R. montanensis*, or PBS
774 (dose 10^5 PFU).
775 (**B**) Spleen weight from injected animals was evaluated at day 7 (n=5).
776 Error bars in (B) represent means ± SEM; from five independent experiments; NS, non-
777 significant; *$p \leq 0.05$; **$p \leq 0.01$.

Fig. 1

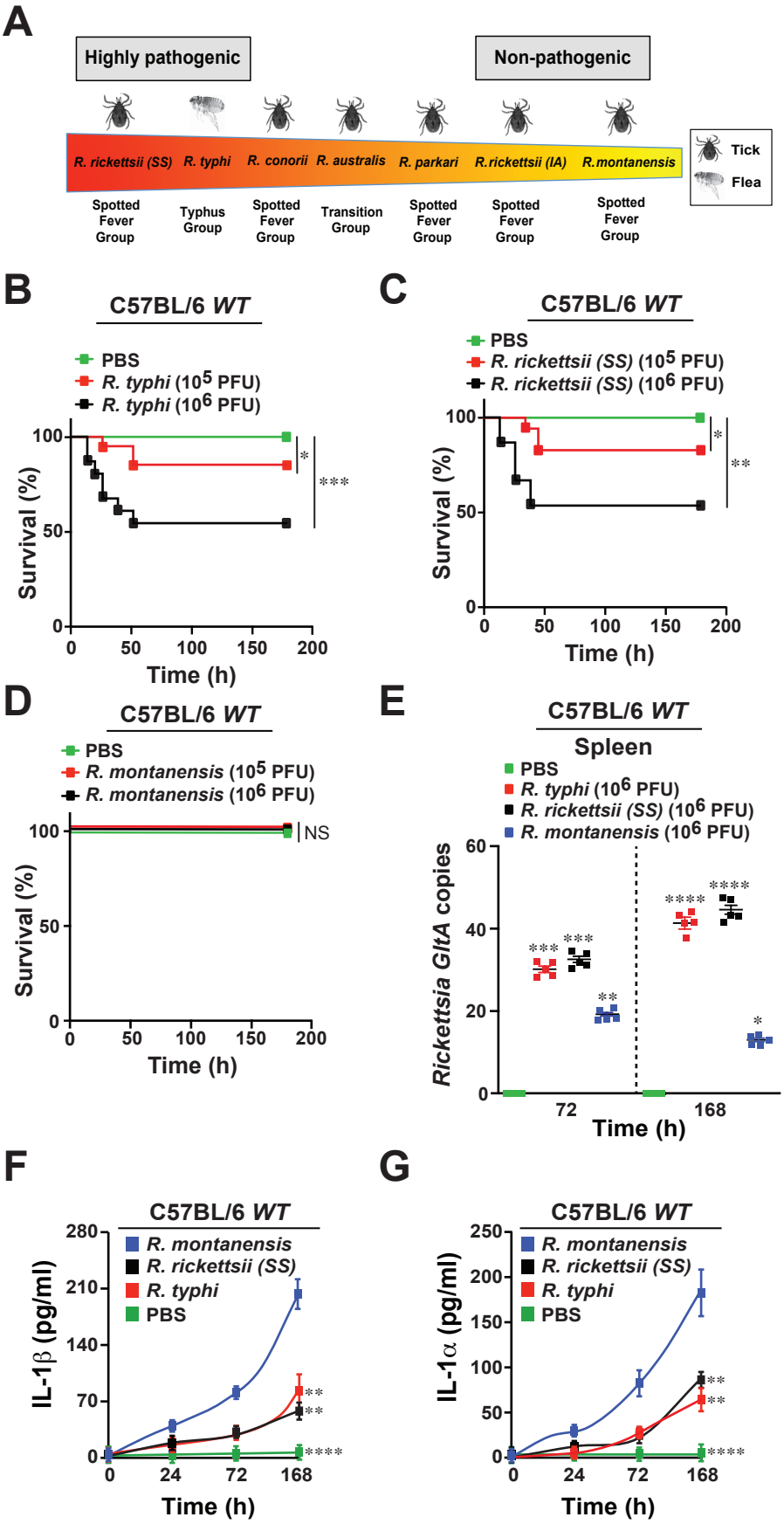
A
Highly pathogenic
Non-pathogenic
R. rickettsii (SS)
R. typhi
R. conorii
R. australis
R. parkari
R.rickettsii (IA)
R.montanensis
Tick
Flea
Spotted Fever Group
Typhus Group
Spotted Fever Group
Transition Group
Spotted Fever Group
Spotted Fever Group
Spotted Fever Group
B
C57BL/6 WT
PBS
R. typhi (10^5 PFU)
R. typhi (10^6 PFU)
Survival (%)
Time (h)
C
C57BL/6 WT
PBS
R. rickettsii (SS) (10^5 PFU)
R. rickettsii (SS) (10^6 PFU)
Survival (%)
Time (h)
D
C57BL/6 WT
PBS
R. montanensis (10^5 PFU)
R. montanensis (10^6 PFU)
NS
Survival (%)
Time (h)
E
C57BL/6 WT
Spleen
PBS
R. typhi (10^6 PFU)
R. rickettsii (SS) (10^6 PFU)
R. montanensis (10^6 PFU)
Rickettsia GltA copies
Time (h)
F
C57BL/6 WT
R. montanensis
R. rickettsii (SS)
R. typhi
PBS
IL-1β (pg/ml)
Time (h)
G
C57BL/6 WT
R. montanensis
R. rickettsii (SS)
R. typhi
PBS
IL-1α (pg/ml)
Time (h)

Fig. 2

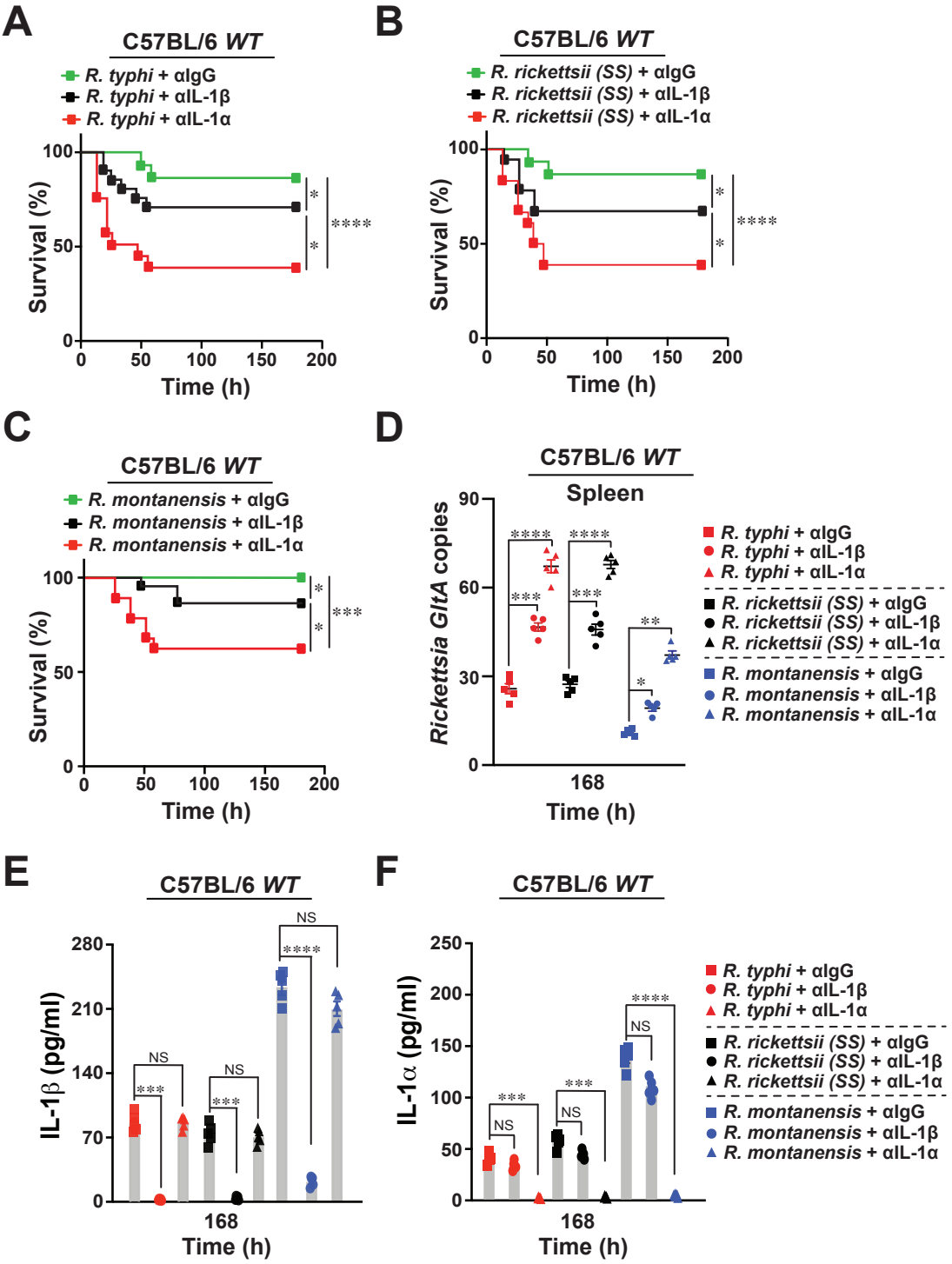
A
C57BL/6 WT
R. typhi + αIgG
R. typhi + αIL-1β
R. typhi + αIL-1α
Survival (%)
Time (h)
B
C57BL/6 WT
R. rickettsii (SS) + αIgG
R. rickettsii (SS) + αIL-1β
R. rickettsii (SS) + αIL-1α
Survival (%)
Time (h)
C
C57BL/6 WT
R. montanensis + αIgG
R. montanensis + αIL-1β
R. montanensis + αIL-1α
Survival (%)
Time (h)
D
C57BL/6 WT
Spleen
Rickettsia GltA copies
168
Time (h)
R. typhi + αIgG
R. typhi + αIL-1β
R. typhi + αIL-1α
R. rickettsii (SS) + αIgG
R. rickettsii (SS) + αIL-1β
R. rickettsii (SS) + αIL-1α
R. montanensis + αIgG
R. montanensis + αIL-1β
R. montanensis + αIL-1α
E
C57BL/6 WT
IL-1β (pg/ml)
168
Time (h)
F
C57BL/6 WT
IL-1α (pg/ml)
168
Time (h)
R. typhi + αIgG
R. typhi + αIL-1β
R. typhi + αIL-1α
R. rickettsii (SS) + αIgG
R. rickettsii (SS) + αIL-1β
R. rickettsii (SS) + αIL-1α
R. montanensis + αIgG
R. montanensis + αIL-1β
R. montanensis + αIL-1α

Fig. 3

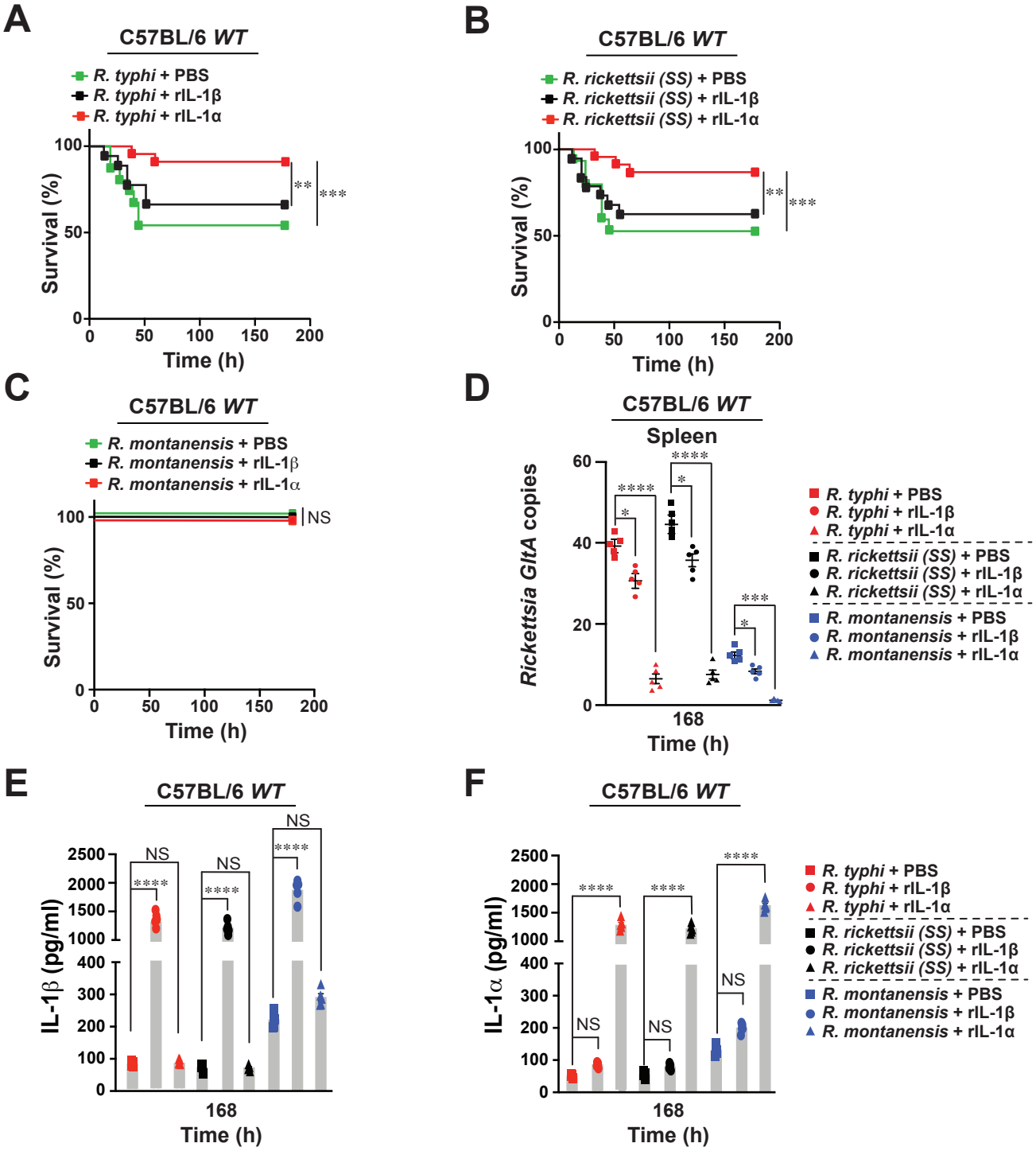
A
C57BL/6 WT
R. typhi + PBS
R. typhi + rIL-1β
R. typhi + rIL-1α
Survival (%)
Time (h)
**
***
B
C57BL/6 WT
R. rickettsii (SS) + PBS
R. rickettsii (SS) + rIL-1β
R. rickettsii (SS) + rIL-1α
Survival (%)
Time (h)
**
***
C
C57BL/6 WT
R. montanensis + PBS
R. montanensis + rIL-1β
R. montanensis + rIL-1α
NS
Survival (%)
Time (h)
D
C57BL/6 WT
Spleen
Rickettsia GltA copies
168
Time (h)
R. typhi + PBS
R. typhi + rIL-1β
R. typhi + rIL-1α
R. rickettsii (SS) + PBS
R. rickettsii (SS) + rIL-1β
R. rickettsii (SS) + rIL-1α
R. montanensis + PBS
R. montanensis + rIL-1β
R. montanensis + rIL-1α
E
C57BL/6 WT
NS
****
IL-1β (pg/ml)
168
Time (h)
F
C57BL/6 WT
****
NS
IL-1α (pg/ml)
168
Time (h)
R. typhi + PBS
R. typhi + rIL-1β
R. typhi + rIL-1α
R. rickettsii (SS) + PBS
R. rickettsii (SS) + rIL-1β
R. rickettsii (SS) + rIL-1α
R. montanensis + PBS
R. montanensis + rIL-1β
R. montanensis + rIL-1α

Fig. 4

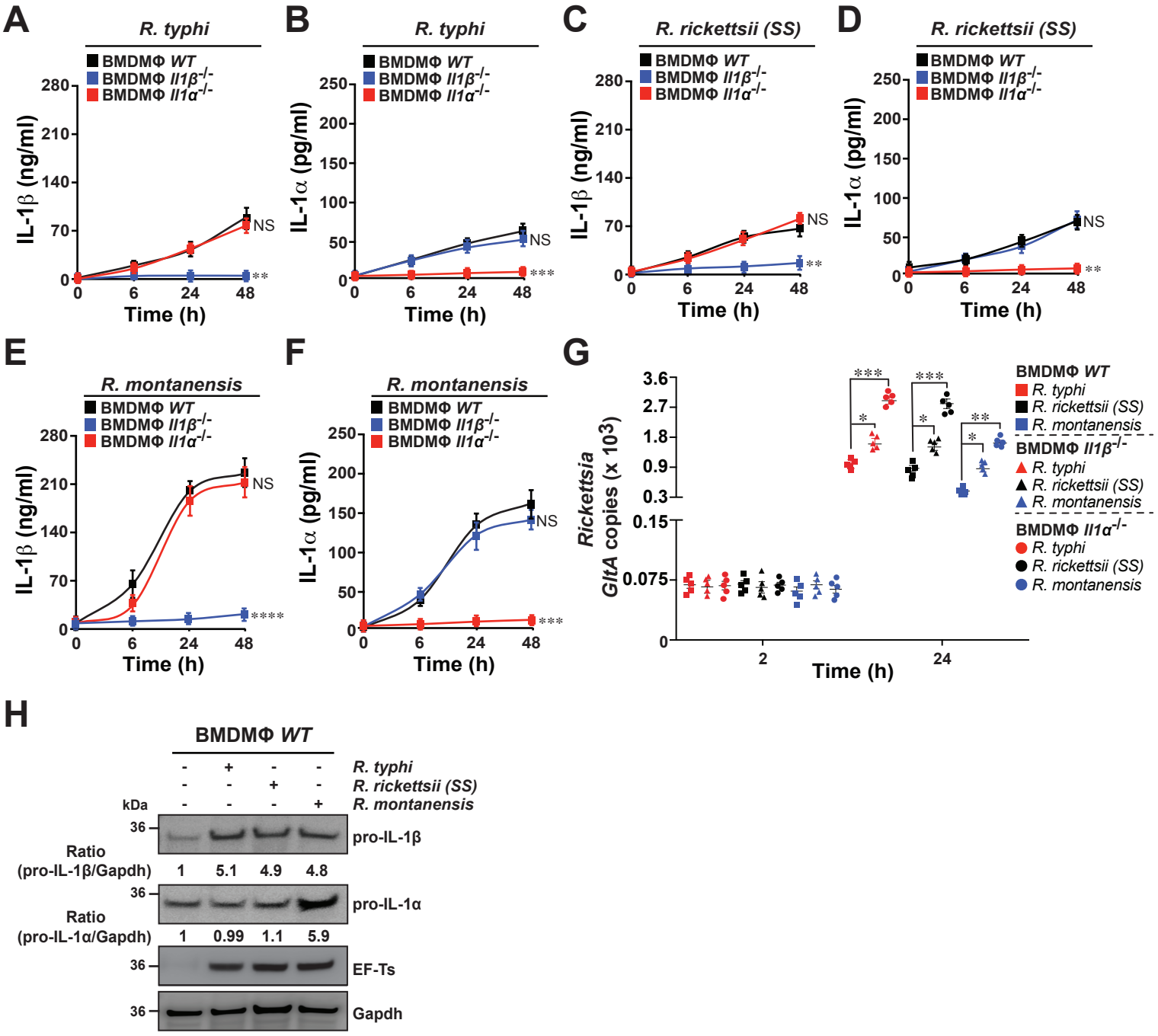
A
R. typhi
BMDMΦ WT
BMDMΦ Il1β-/-
BMDMΦ Il1α-/-
IL-1β (ng/ml)
Time (h)
NS
**
B
R. typhi
IL-1α (pg/ml)
NS
***
C
R. rickettsii (SS)
IL-1β (ng/ml)
NS
**
D
R. rickettsii (SS)
IL-1α (pg/ml)
NS
**
E
R. montanensis
IL-1β (ng/ml)
NS
****
F
R. montanensis
IL-1α (pg/ml)
NS
***
G
Rickettsia GltA copies (x 10^3)
Time (h)
BMDMΦ WT
R. typhi
R. rickettsii (SS)
R. montanensis
BMDMΦ Il1β-/-
R. typhi
R. rickettsii (SS)
R. montanensis
BMDMΦ Il1α-/-
R. typhi
R. rickettsii (SS)
R. montanensis

H
BMDMΦ WT
R. typhi
R. rickettsii (SS)
R. montanensis
kDa
pro-IL-1β
Ratio (pro-IL-1β/Gapdh) 1 5.1 4.9 4.8
pro-IL-1α
Ratio (pro-IL-1α/Gapdh) 1 0.99 1.1 5.9
EF-Ts
Gapdh

Fig. 5

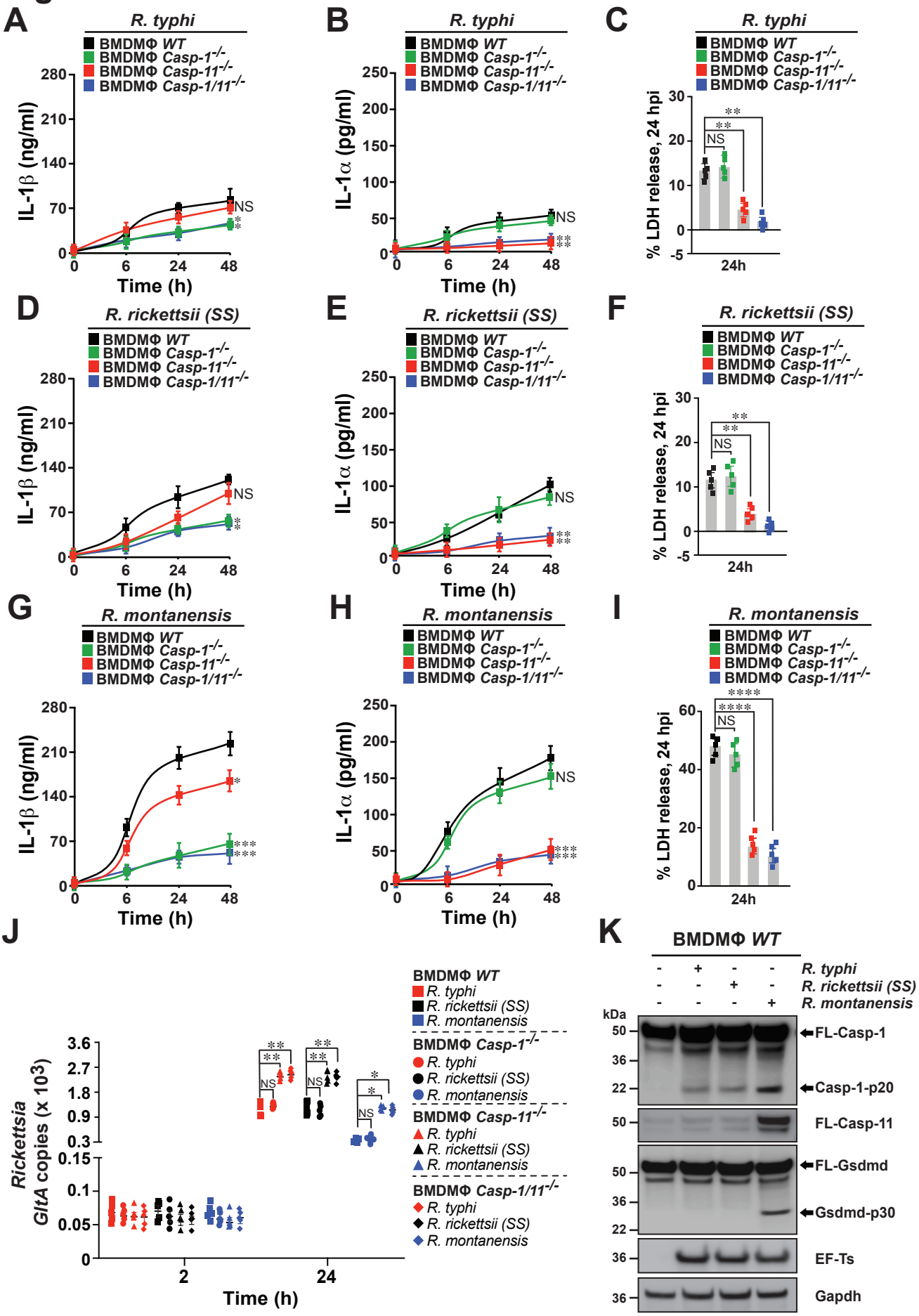
A
R. typhi
BMDMΦ WT
BMDMΦ Casp-1-/-
BMDMΦ Casp-11-/-
BMDMΦ Casp-1/11-/-
IL-1β (ng/ml)
Time (h)
B
IL-1α (pg/ml)
C
% LDH release, 24 hpi
24h
D
R. rickettsii (SS)
E
F
G
R. montanensis
H
I
J
Rickettsia GltA copies (x 10^3)
BMDMΦ WT
R. typhi
R. rickettsii (SS)
R. montanensis
BMDMΦ Casp-1-/-
BMDMΦ Casp-11-/-
BMDMΦ Casp-1/11-/-
K
BMDMΦ WT
R. typhi
R. rickettsii (SS)
R. montanensis
kDa
FL-Casp-1
Casp-1-p20
FL-Casp-11
FL-Gsdmd
Gsdmd-p30
EF-Ts
Gapdh

Fig. 6

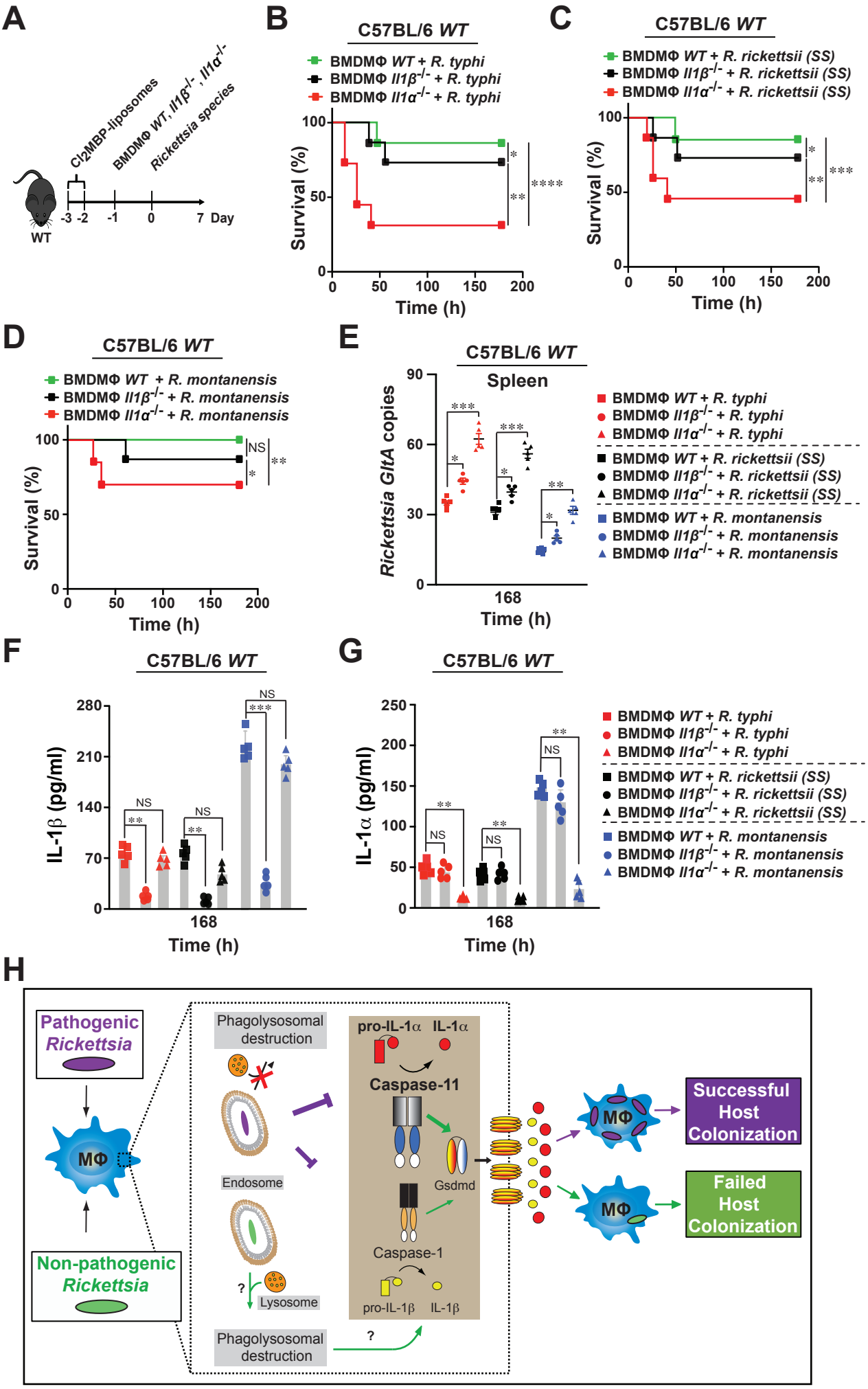
A
Cl2MBP-liposomes
BMDMΦ WT, Il1β-/-, Il1α-/-
Rickettsia species
WT
-3 -2 -1 0 7 Day
B
C57BL/6 WT
BMDMΦ WT + R. typhi
BMDMΦ Il1β-/- + R. typhi
BMDMΦ Il1α-/- + R. typhi
Survival (%)
Time (h)
C
C57BL/6 WT
BMDMΦ WT + R. rickettsii (SS)
BMDMΦ Il1β-/- + R. rickettsii (SS)
BMDMΦ Il1α-/- + R. rickettsii (SS)
Survival (%)
Time (h)
D
C57BL/6 WT
BMDMΦ WT + R. montanensis
BMDMΦ Il1β-/- + R. montanensis
BMDMΦ Il1α-/- + R. montanensis
Survival (%)
Time (h)
E
C57BL/6 WT
Spleen
Rickettsia GltA copies
168
Time (h)
BMDMΦ WT + R. typhi
BMDMΦ Il1β-/- + R. typhi
BMDMΦ Il1α-/- + R. typhi
BMDMΦ WT + R. rickettsii (SS)
BMDMΦ Il1β-/- + R. rickettsii (SS)
BMDMΦ Il1α-/- + R. rickettsii (SS)
BMDMΦ WT + R. montanensis
BMDMΦ Il1β-/- + R. montanensis
BMDMΦ Il1α-/- + R. montanensis
F
C57BL/6 WT
IL-1β (pg/ml)
168
Time (h)
G
C57BL/6 WT
IL-1α (pg/ml)
168
Time (h)
BMDMΦ WT + R. typhi
BMDMΦ Il1β-/- + R. typhi
BMDMΦ Il1α-/- + R. typhi
BMDMΦ WT + R. rickettsii (SS)
BMDMΦ Il1β-/- + R. rickettsii (SS)
BMDMΦ Il1α-/- + R. rickettsii (SS)
BMDMΦ WT + R. montanensis
BMDMΦ Il1β-/- + R. montanensis
BMDMΦ Il1α-/- + R. montanensis
H
Pathogenic Rickettsia
MΦ
Non-pathogenic Rickettsia
Phagolysosomal destruction
Endosome
Lysosome
Phagolysosomal destruction
pro-IL-1α
IL-1α
Caspase-11
Gsdmd
Caspase-1
pro-IL-1β
IL-1β
MΦ
MΦ
Successful Host Colonization
Failed Host Colonization

Fig. S1

A

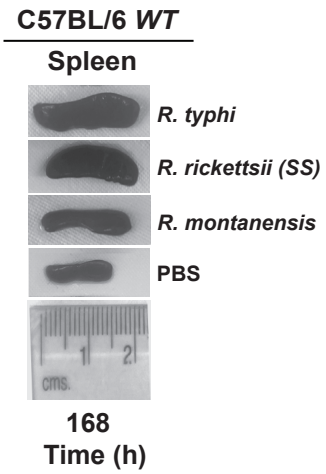
C57BL/6 WT
Spleen
R. typhi
R. rickettsii (SS)
R. montanensis
PBS
cms.
168
Time (h)

B

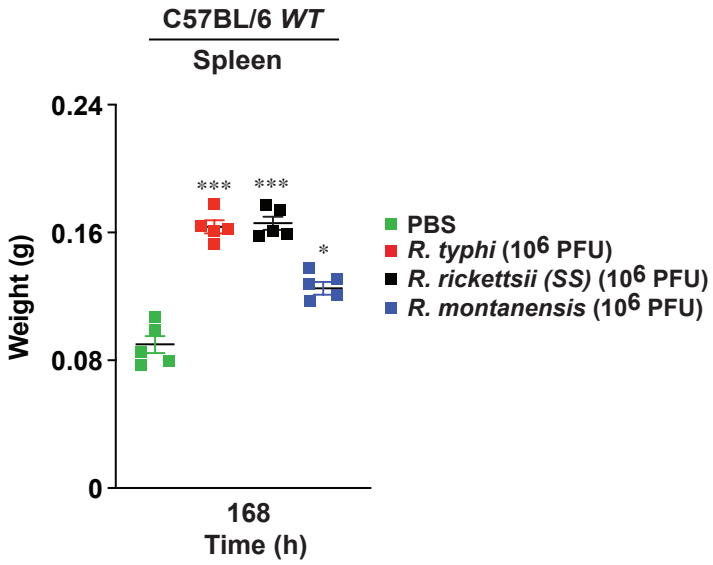
C57BL/6 WT
Spleen
Weight (g)
0.24
0.16
0.08
0
***
***
*
168
Time (h)
PBS
R. typhi (10^6 PFU)
R. rickettsii (SS) (10^6 PFU)
R. montanensis (10^6 PFU)

Fig. S2

A

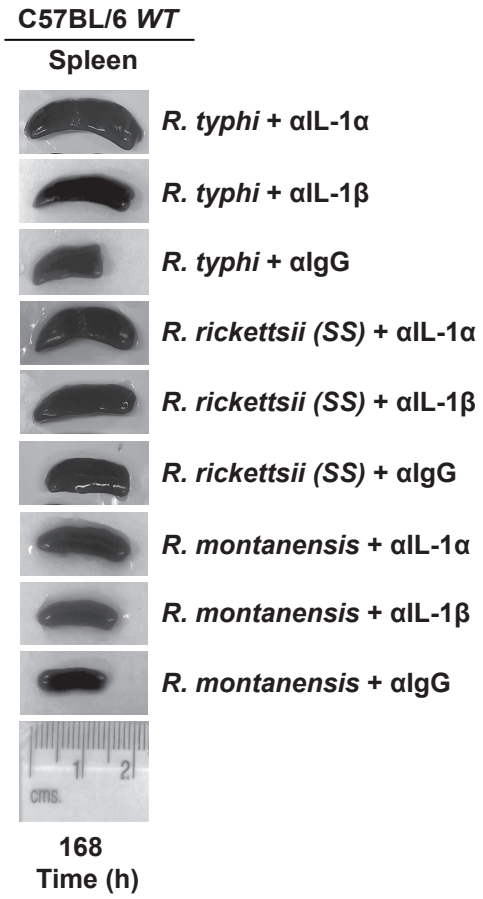
C57BL/6 WT
Spleen
R. typhi + αIL-1α
R. typhi + αIL-1β
R. typhi + αIgG
R. rickettsii (SS) + αIL-1α
R. rickettsii (SS) + αIL-1β
R. rickettsii (SS) + αIgG
R. montanensis + αIL-1α
R. montanensis + αIL-1β
R. montanensis + αIgG
cms.
168
Time (h)

B

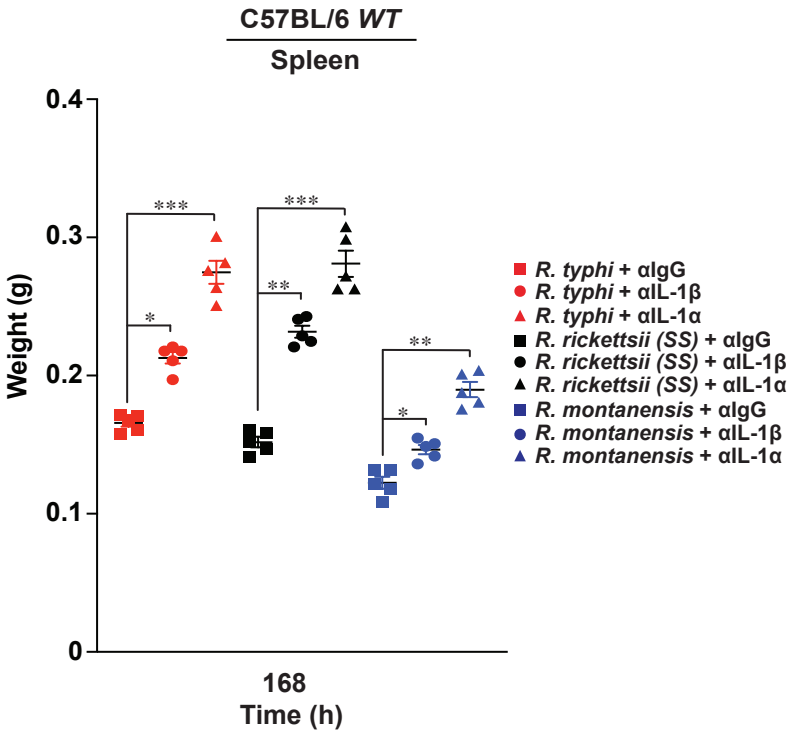
C57BL/6 WT
Spleen
Weight (g)
0.4
0.3
0.2
0.1
0
***
***
*
**
**
*
168
Time (h)
R. typhi + αIgG
R. typhi + αIL-1β
R. typhi + αIL-1α
R. rickettsii (SS) + αIgG
R. rickettsii (SS) + αIL-1β
R. rickettsii (SS) + αIL-1α
R. montanensis + αIgG
R. montanensis + αIL-1β
R. montanensis + αIL-1α

Fig. S3

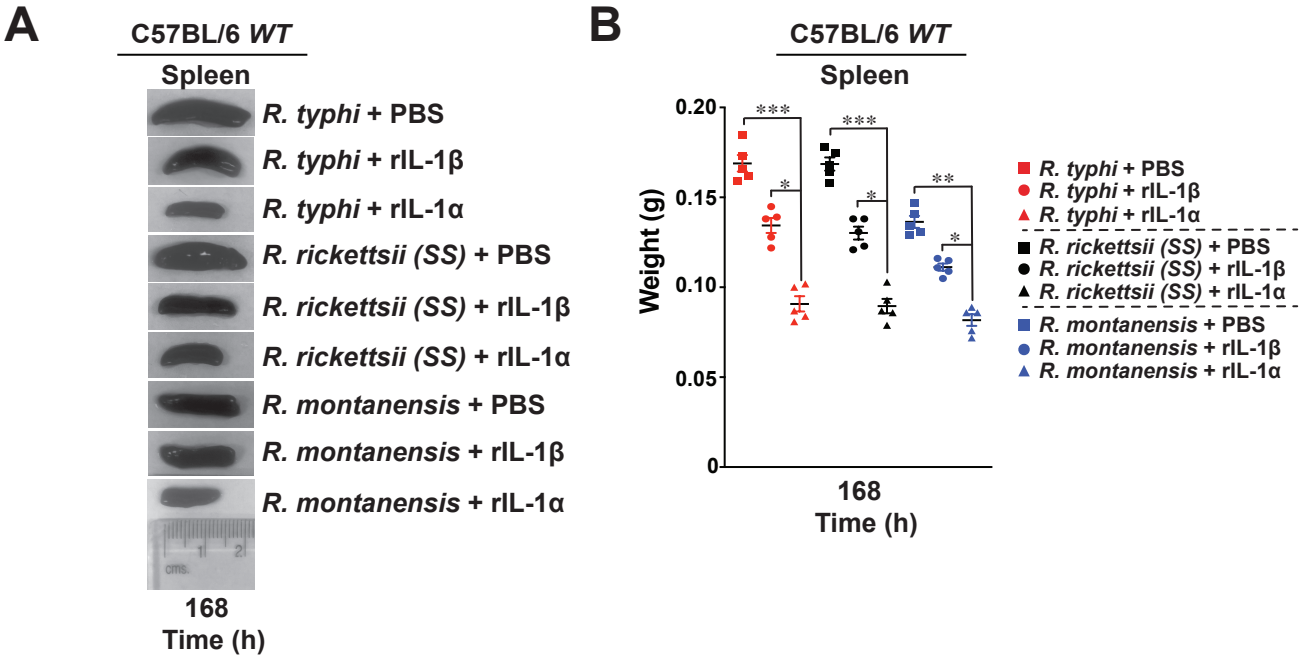
A
C57BL/6 WT
Spleen
R. typhi + PBS
R. typhi + rIL-1β
R. typhi + rIL-1α
R. rickettsii (SS) + PBS
R. rickettsii (SS) + rIL-1β
R. rickettsii (SS) + rIL-1α
R. montanensis + PBS
R. montanensis + rIL-1β
R. montanensis + rIL-1α
168
Time (h)
B
C57BL/6 WT
Spleen
Weight (g)
0.20
0.15
0.10
0.05
0
***
*
***
*
**
*
168
Time (h)
R. typhi + PBS
R. typhi + rIL-1β
R. typhi + rIL-1α
R. rickettsii (SS) + PBS
R. rickettsii (SS) + rIL-1β
R. rickettsii (SS) + rIL-1α
R. montanensis + PBS
R. montanensis + rIL-1β
R. montanensis + rIL-1α

Fig. S4

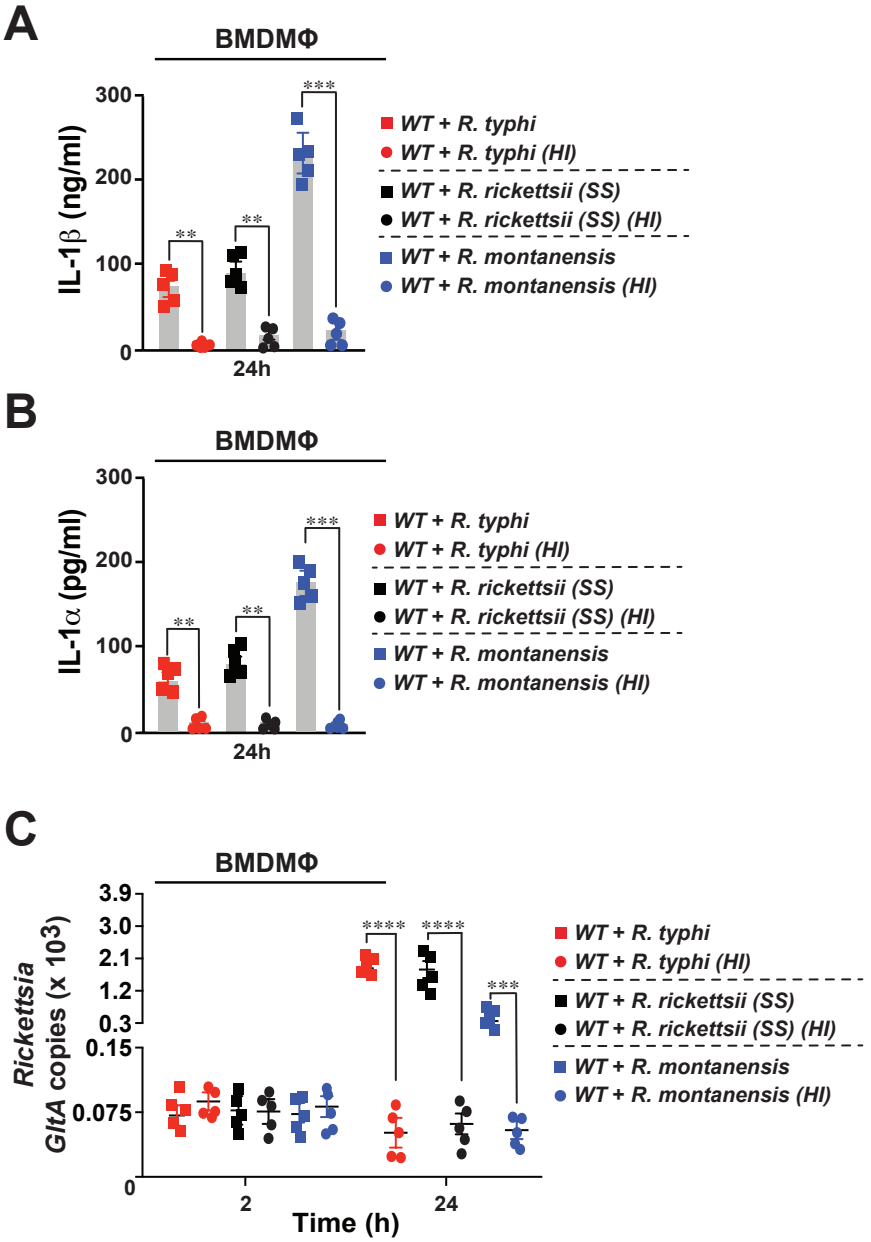
A
BMDMΦ
IL-1β (ng/ml)
300
200
100
0
24h
**
**
***
WT + R. typhi
WT + R. typhi (HI)
WT + R. rickettsii (SS)
WT + R. rickettsii (SS) (HI)
WT + R. montanensis
WT + R. montanensis (HI)
B
BMDMΦ
IL-1α (pg/ml)
300
200
100
0
24h
**
**
***
WT + R. typhi
WT + R. typhi (HI)
WT + R. rickettsii (SS)
WT + R. rickettsii (SS) (HI)
WT + R. montanensis
WT + R. montanensis (HI)
C
BMDMΦ
Rickettsia GltA copies (x 10³)
3.9
3.0
2.1
1.2
0.3
0.15
0.075
0
2
24
Time (h)
****
****
***
WT + R. typhi
WT + R. typhi (HI)
WT + R. rickettsii (SS)
WT + R. rickettsii (SS) (HI)
WT + R. montanensis
WT + R. montanensis (HI)

Fig. S5

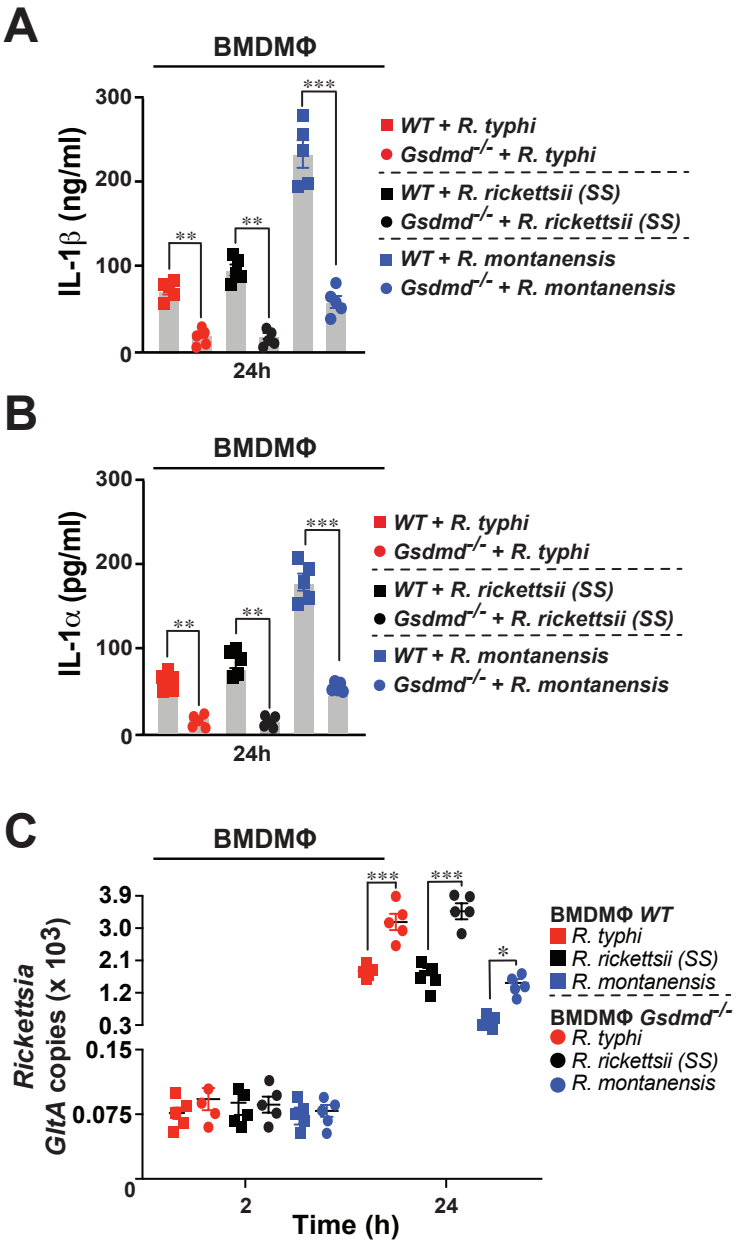
A
BMDMΦ
IL-1β (ng/ml)
300
200
100
0
24h
**
**
***
WT + R. typhi
Gsdmd-/- + R. typhi
WT + R. rickettsii (SS)
Gsdmd-/- + R. rickettsii (SS)
WT + R. montanensis
Gsdmd-/- + R. montanensis
B
BMDMΦ
IL-1α (pg/ml)
300
200
100
0
24h
**
**
***
WT + R. typhi
Gsdmd-/- + R. typhi
WT + R. rickettsii (SS)
Gsdmd-/- + R. rickettsii (SS)
WT + R. montanensis
Gsdmd-/- + R. montanensis
C
BMDMΦ
Rickettsia GltA copies (x 10^3)
3.9
3.0
2.1
1.2
0.3
0.15
0.075
0
2
24
Time (h)
***
***
*
BMDMΦ WT
R. typhi
R. rickettsii (SS)
R. montanensis
BMDMΦ Gsdmd-/-
R. typhi
R. rickettsii (SS)
R. montanensis

Fig. S6

A

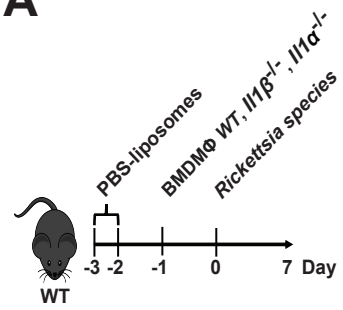
PBS-liposomes
BMDMΦ WT, Il1β-/-, Il1α-/-
Rickettsia species
-3 -2 -1 0 7 Day
WT

B

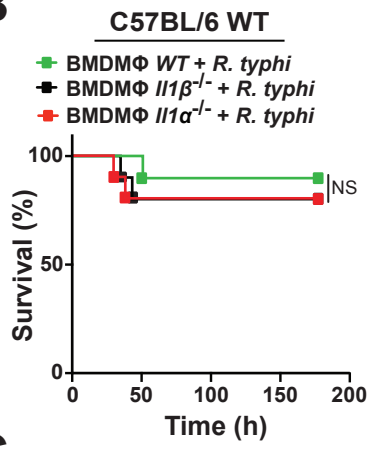
C57BL/6 WT
BMDMΦ WT + R. typhi
BMDMΦ Il1β-/- + R. typhi
BMDMΦ Il1α-/- + R. typhi
NS
Survival (%)
100
50
0
0 50 100 150 200
Time (h)

C

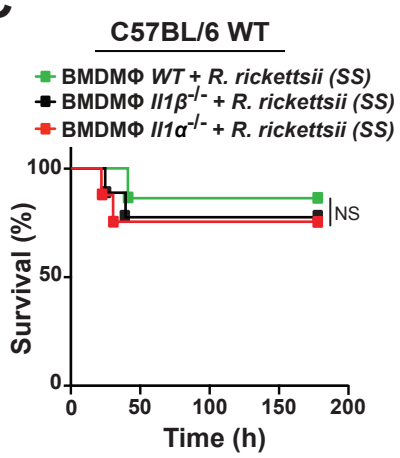
C57BL/6 WT
BMDMΦ WT + R. rickettsii (SS)
BMDMΦ Il1β-/- + R. rickettsii (SS)
BMDMΦ Il1α-/- + R. rickettsii (SS)
NS
Survival (%)
100
50
0
0 50 100 150 200
Time (h)

D

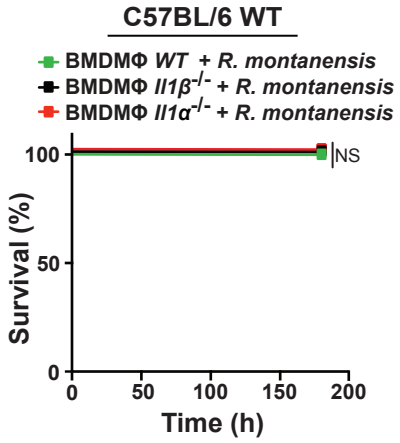
C57BL/6 WT
BMDMΦ WT + R. montanensis
BMDMΦ Il1β-/- + R. montanensis
BMDMΦ Il1α-/- + R. montanensis
NS
Survival (%)
100
50
0
0 50 100 150 200
Time (h)

Fig. S7

A

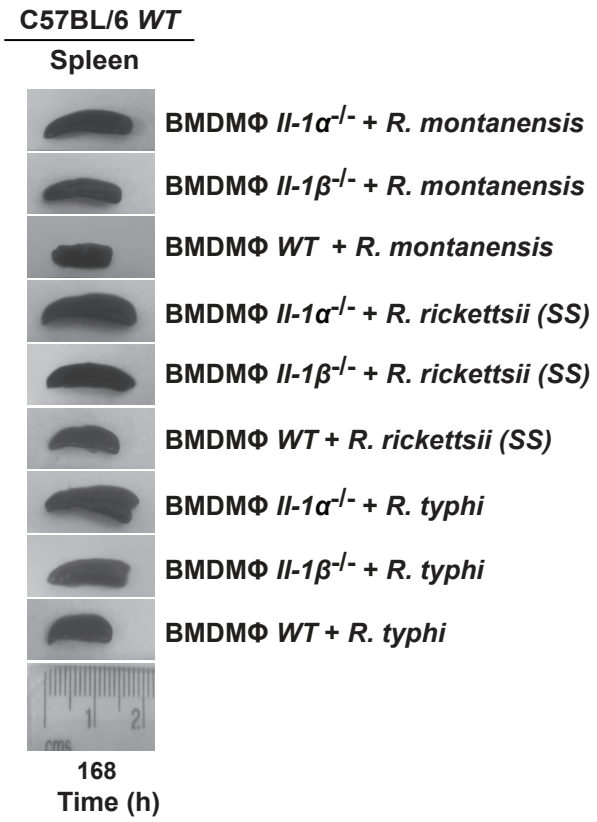
C57BL/6 WT
Spleen
BMDMΦ Il-1α-/- + R. montanensis
BMDMΦ Il-1β-/- + R. montanensis
BMDMΦ WT + R. montanensis
BMDMΦ Il-1α-/- + R. rickettsii (SS)
BMDMΦ Il-1β-/- + R. rickettsii (SS)
BMDMΦ WT + R. rickettsii (SS)
BMDMΦ Il-1α-/- + R. typhi
BMDMΦ Il-1β-/- + R. typhi
BMDMΦ WT + R. typhi
168
Time (h)

B

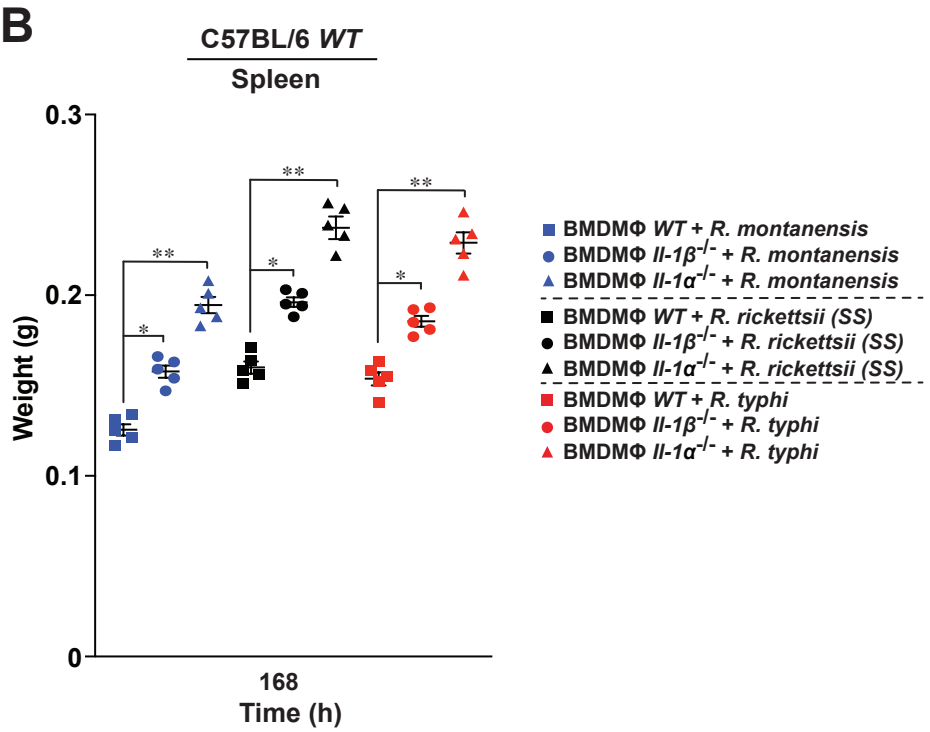
C57BL/6 WT
Spleen
0.3
0.2
0.1
0
Weight (g)
**
*
168
Time (h)
BMDMΦ WT + R. montanensis
BMDMΦ Il-1β-/- + R. montanensis
BMDMΦ Il-1α-/- + R. montanensis
BMDMΦ WT + R. rickettsii (SS)
BMDMΦ Il-1β-/- + R. rickettsii (SS)
BMDMΦ Il-1α-/- + R. rickettsii (SS)
BMDMΦ WT + R. typhi
BMDMΦ Il-1β-/- + R. typhi
BMDMΦ Il-1α-/- + R. typhi